NUMERICAL MODELLING OF POWER TRANSFORMERS UNDER GEOMAGNETICALLY INDUCED CURRENTS

A thesis submitted to the Delft University of Technology in partial fulfillment
of the requirements for the degree of

Master of Science in Electrical Power Engineering

by

Deeksha Venkatesh
Student no. 5012554

August 2021

Thesis committee: Dr. Peter Vaessen, TU Delft Supervisor
Dr. Simon Tindemans
Dr. Mohamad Ghaffarian Niasar , TU Delft Daily Supervisor
Ir. Bart Simons, Royal Smit Transformers Company Supervisor

ABSTRACT

Modelling of power transformers to predict and examine its performance in the presence of Geomagnetic Induced Currents (GICs) is of particular interest in research since these currents that are quasi-DC in nature drive the transformer into half-cycle saturation. During the half-cycle saturation, the increased leakage flux and harmonics have undesirable effects on the windings and the structural components of the transformer, which can possibly lead to their permanent damage. This prompts the need to perform a precautionary study of the transformer validating its robustness when subject to GICs.

This thesis proposes a method to model the transformer and its electromagnetic (EM) behaviour under GICs that combines the accuracy of Finite Element Modelling (FEM) with the speed of Magnetic Equivalent Modelling (MEM) to produce a fast-computing yet detailed modelling method using simulation tools, COMSOL and MATLAB Simulink, respectively. The transformer under study in this thesis is a single-phase 280MVA, 500/230kV auto transformer designed by Royal Smit Transformers. It was first modelled using FEM in COMSOL, providing details of the equivalent 2D axisymmetric geometry of the core and the windings and the material properties to each component. The model was then computed and validated against factory measurements done by Royal SMIT for the transformer when not subjected to GICs. After which, the model was run for the condition in which the transformer is subject to a GIC. The main problem of failure of the model to converge before reaching steady-state condition under GIC was overcome after optimizing the solver settings of the FEM software. The difference in the EM behaviour of the transformer with and without GIC were studied.

After ensuring that the FEM model was robust and accurately represents the transformer under GIC as well, the time-consuming part of computing the FEM model till it reached steady-state under GIC was then made to be taken care of by a MEM model developed in Simulink. Induced flux versus magnetizing current characteristics of the transformer were obtained from the FEM model, and fed to the MEM model, which only took a few seconds to run. The magnetizing current waveform obtained for a few cycles after reaching steady-state under GIC was then transferred to the FEM model, which could finally compute - for those values of magnetizing current - the detailed EM effects of GICs on the transformer, spatially.

An important EM study needing the spatial distribution of the EM properties within the transformer is the calculation of eddy current losses in the windings. In this thesis, a method that only considers the envelope of the set of windings as opposed to modelling every strand to calculate their losses is developed using an analytical formula found in literature. This is validated against the losses calculated by Royal SMIT as well as the FEM software for a detailed model of the windings.

The timesaving method to study the EM behaviour of transformers subject to GIC proposed in this thesis accurately models the transformer in the saturation region that should enable conducting EM studies furthermore to winding loss calculation with ease.

ACKNOWLEDGEMENTS

In the length of time that has culminated in this master thesis, I have many to be grateful for. Achieving this feat was certainly a challenge in more ways than one. Through it all, there have been a few who stand out and unconditionally meant well for me, with their unwavering support; and I'm thankful to have crossed paths with them in this duration.

My sincerest gratitude to Dr. Peter Vaessen for being my supervisor, whose knowledge and expertise in the field of High Voltage Technology I have been in awe of and have had the privilege of witnessing. I would, then, like to thank my daily university supervisor, Dr. M. Ghaffarian Niasar for being an affirming and guiding light through my masters career, and for offering help without hesitation through my bouts of uncertainties with warmth and ease. His palpable excitement for his field of study, High Voltage Technology and his eagerness to take on a relatively new arena within that field with my thesis, certainly made my desire for them grow as well. I would, then, like to extend my gratitude to the university, TU Delft, and DC Systems, Energy Conversion Storage Group within its Faculty of EEMCS for providing me this opportunity to conduct research to my heart's content, for enabling me to hone my inquisitive research skills, through the expertise of its faculty. I would also like to take this moment to thank Dr. Simon Tindemans, for agreeing to be on my defense committee to evaluate my thesis.

An opportunity to work on an exciting topic such as this wouldn't have been possible if my daily company supervisor, Ir. Bart Simons from Royal Smit Transformers, hadn't offered it when I approached them. Agreeing to the project and him as my supervisor has been nothing short of rewarding, as he patiently guided me with his geniality as I waded my way through the world of transformers, and for that I am extremely grateful. Next, I have Dr. Ir. Timo Overboom from Royal Smit Transformers to be thankful for. His technical know-how paired with his enthusiasm for the topic made brainstorming sessions with him a delight, and his valuable insights every step of the way through this thesis has made it what it is now.

I would like to conclude with my eternal gratitude towards my mother and grandmother, the beginning to my everything, for remaining my role-models for perseverance and strength. This thesis has brought me closer to them, as they went the extra mile to be my anchor and offered me moral support at times when my endurance was tested and helped overcome struggles with myself, even when miles apart. On that note, a little post script extension of gratitude to my friends back home who never fail to light up my day and those in the Netherlands who make me feel at home away from home.

Thank you to everyone mentioned above for making this journey at TU Delft more enjoyable.

CONTENTS

LIST OF FIGURES

LIST OF TABLES

1 INTRODUCTION

Geomagnetic induced currents (GICs) occur in a power system when solar flares interact with Earth's magnetic field [8]. Solar flares emit large amounts of charged particles erupting from a sunspot group on the Sun's surface of high magnetic flux concentration. This happens in accordance with the 11-year solar cycle. Depending on the initial velocity and trajectory, it may take 20 to 40 hours after the solar flare for the geomagnetic field to capture the emitted charged particles. This interaction causes transient fluctuations in the Earth's magnetic field causing a geomagnetic disturbance lasting for periods in the order of several minutes (refer Fig. 1.1).

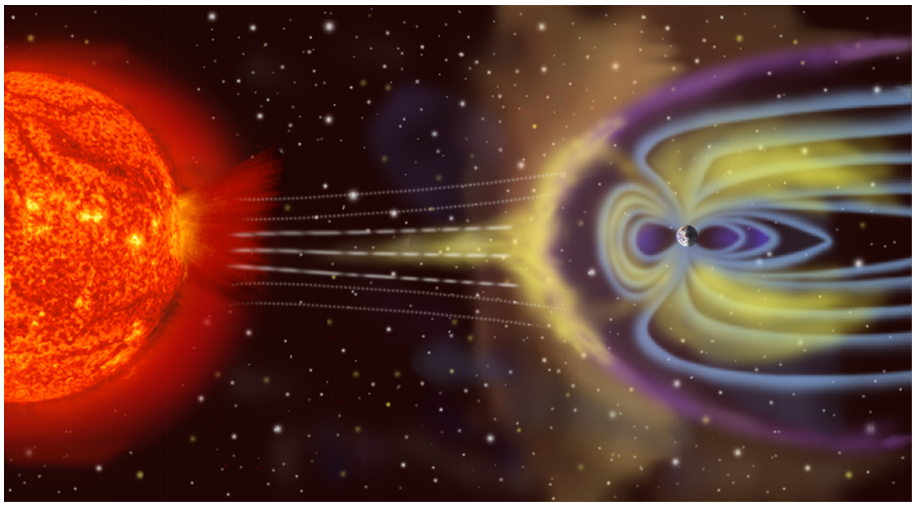

Figure 1.1: Solar storm interacting with Earth's magnetic field [2]

These fluctuations induce earth-surface electric fields of the order of 3-6 V/km [4]. Across long transmission lines between power system grounding points, these electric fields can result in a huge potential difference, allowing slowly-varying zero-sequence quasi-DC currents, i.e. GICs, of magnitudes typically of tens of amperes up to maximum 200A to flow through the system [9].

In concern with power transformers, GIC travels through their grounded neutrals and the quasi-DC current can drive the core of the transformer into half-cycle saturation – the phenomenon causing a number of adverse problems. Undesirable effects due to saturation include rise in stray flux and introduction of even and odd harmonics through the magnetizing current which leads to (local) overheating of windings of the transformers, as well as its structural parts such as core and winding clamps, flux shields, tank walls, etc. resulting in accelerated ageing of insulation, high amount of vibrations and sound as well as voltage drop distortions across secondary terminals. These conditions, in turn, from the point of view of the power system, result in increase in reactive power demand, voltage instability, symmetric energy phase transport across the transformer, and maloperation of protective relays [4]. It, thus, becomes imperative to emulate the phenomena of GIC in power transformers and assess the extent of damages incurred due to different levels of GIC.

1.1 THEORY

1.1.1 Principle of Transformers [1]

Transformers are AC electrical machines, falling under the category of transducers, that transfer electric energy from one circuit to another without any change in frequency. They are used to step up or step-down AC voltages in a power system. They step up the voltages of magnitudes 15-20kV generated by power plants to transmit over long distances effectively reducing the transmission I^2R losses for a given amount of power. They also step-down voltages at the distribution level of the power system for residential, industrial and commercial use of electrical energy.

A transformer performs electrical energy transfer through the principle of electromagnetic induction, wherein it consists of two electrically conducting windings called primary and secondary windings that are magnetically coupled via a highly permeable core, and are either electrically isolated from one another as in the case of a full transformer or electrically connected as in the case of auto-transformer which is about 60% of the production at Royal Smit Transformers. The core provides a very low reluctance path for the magnetic flux induced.

When a voltage (V) is applied on the primary side of the transformer with an open circuit (no-load) on the secondary side, a flux is induced in the core proportional to the integration of applied voltage, according to Faraday's law of induction. The core has much higher magnetic permeability than air, thus the flux induced chooses to flow through the core than air. This flux links the primary and the secondary windings (assuming no leakage flux). Thus, according to Faraday's law of induction, this changing flux in the core induces a voltage across the primary winding terminals,

$$e_1(t) = N_1 \frac{d\phi_m(t)}{dt}, \tag{1.1}$$

where $\phi_m(t)$ is the mutual linking flux. Ignoring winding resistance and its leakage inductance, the voltage induced across the terminals must equal the supply voltage. Thus,

$$v_p(t) = e_p(t), \tag{1.2}$$

If $\phi_{mp}(t) = \phi_{mp} sin\omega t$, where ϕ_{mp} is the peak mutual flux,

$$v_1(t) = e_1(t) = N_1 \omega \phi_{mp} cos\omega t, \tag{1.3}$$

and their root mean square (RMS) values would be

$$E_1 = \frac{(N_1 \omega \phi_{mp})}{\sqrt{2}} = 4.44 \phi_{mp} f N_1. \tag{1.4}$$

This is known as the EMF equation of the transformer. Similarly, the mutual flux induces a voltage across the secondary winding terminals,

$$e_2(t) = N_2 \frac{d\phi_m(t))}{dt} \tag{1.5}$$

and

$$E_2 = 4.44 \phi_{mp} f N_2. \tag{1.6}$$

Under no-load condition, the excitation current drawn by the primary is just the magnetizing current ($I_1 = I_m$) which is in phase with the mutual flux, if eddy losses and hysteresis of the core are ignored.

If a load is now connected across the secondary, a current flows through it whose magneto-motive force (I_2N_2) tries to oppose the mutual flux flowing through the solenoid according to Lenz's law. But in an ideal transformer, if the supply voltage is constant, the induced voltage as well the mutual flux must be constant. This implies that the primary must draw additional current ($I_1^{'}$) compensating for the demagnetizing effect of the secondary's mmf. Thus,

$$I_1^{'}N_1 = I_2N_2 \tag{1.7}$$

Vectorially, the total primary current drawn becomes

$$\vec{I_1} = \vec{I_1}^{'} + \vec{I_m}. \tag{1.8}$$

Relating primary induced EMFs and currents to those of secondary and knowing that power transferred across an ideal transformer is lossless (i.e. $V_1I_1 = V_2I_2$), we obtain,

$$E_1/E_2 = I_2/I_1 = N_1/N_2 = a \tag{1.9}$$

where a is known as the transformation ratio.

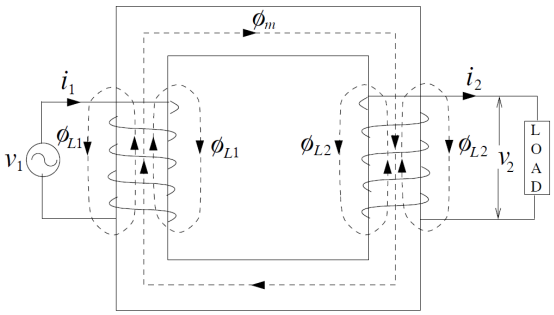

Figure 1.2: Practical transformer [1]

In a practical transformer (Fig. 1.2), there are eddy current and hysteresis losses present in the core, and so are winding resistance losses and leakage field losses in the windings. The equivalent circuit including representation of the above around an ideal transformer is shown in Fig. 1.3. R_1 and R_2 represent the primary and secondary winding resistances, respectively. Leakage flux corresponding to a winding is that part of the total flux induced by the winding that doesn't link the primary to the secondary and is exclusive to the winding producing the flux. X_{L1} and X_{L2} represent the inductive reactance associated with the voltage drop due to the leakage flux produced by the primary and secondary windings, respectively. These resistances and reactances are connected in series to their respective winding as they are in phase with the current through them, because their magnetic flux paths are mainly through air which doesn't have hysteresis.

In a practical transformer, the no-load exciting current consists of, in addition to the magnetizing component contributing to and in phase with the mutual flux (I_m), the core-loss component (I_c) accounting for the eddy current and hysteresis losses in the core which is in phase with the induced voltage. Thus, vectorially,

$$\vec{I_0} = \vec{I_m} + \vec{I_c} \tag{1.10}$$

$$\vec{I_1} = \vec{I_1}^{'} + \vec{I_m} + \vec{I_c}. \tag{1.11}$$

The voltage drops due to the magnetizing component and the core-loss component are taken care of by the non-linear reactance X_m and resistor R_c, respectively, in a shunt branch on the primary side since these core losses are always present regardless of the presence of a load.

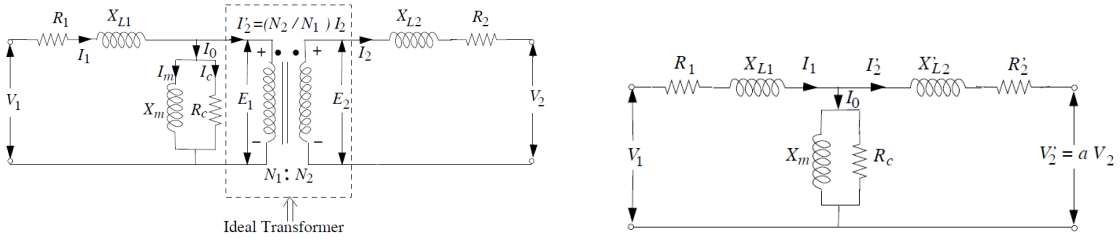

(a) Before referred to any side

(b) After referred to primary side

Figure 1.3: Equivalent circuit of a transformer [1]

The EMF equations for such an equivalent circuit of a transformer thus becomes,

$$V_1 = E_1 + I_1(R_1 + X_{L1}) \tag{1.12}$$

$$V_2 = E_2 - I_2(R_2 + X_{L2}) \tag{1.13}$$

In order to remove the ideal transformer in the equivalent circuit and refer all quantities completely to primary side, one can replace the secondary winding with one that has the same number of turns as the primary so that the voltage across both the windings are now the same and the ideal transformer can be eliminated. But it must be ensured that the power drop across all elements of the secondary remains the same. Thus,

$$R_2^{'} = R_2(\frac{I_2}{I_1^{'}})^2 = R_s(\frac{N_1 I_2}{N_2 I_2})^2 = a^2 R_2. \tag{1.14}$$

Similarly,

$$X_L 2^{'} = a^2 X_L 2, \tag{1.15}$$

and

$$V_2^{'} = aV_2 \tag{1.16}$$

Similarly, equivalent circuit can be figured completely referring all elements to the secondary side.

1.1.2 Saturation Effects

If core-losses are ignored, the shape of the magnetizing current waveform and that of the magnetic flux density depends on the shape of the B-H relationship of the core. Most transformer cores are made of soft ferromagnetic material which has a linear B-H curve until a certain point called knee point beyond which it saturates. For a given frequency, the rated voltage of a transformer corresponds to that that enables the transformer to operate around the knee point of the B-H curve.

For a transformer operating in the linear region of the BH-curve, the magnetic flux density waveforms is proportional to the magnetizing current that determines the magnetic field intensity and they are of pure sinusoidal nature. When a transformer is thus overexcited, i.e., supplied more than the rated voltage, the proportional flux density induced would have values lying in the saturation region of the B-H curve of the core. Thus, the magnetic field and therefore, the magnetizing current waveforms take on a peaky nature rich in odd harmonics due to half-wave symmetry, with the 3rd harmonic being the predominant one in addition to the fundamental component.

Under application of a DC voltage along with the rated supply AC voltage to the transformer under no-load – the circuit of which can be assumed to be represented by a non-linear inductor in series with a resistor - the flux induced which is proportional to the DC+AC voltage has a steadily increasing offset. This implies, that the half-cycle with the crests of the waveform is pushed increasingly into the saturation region of the B-H curve of the core, as shown in Fig. 1.4.

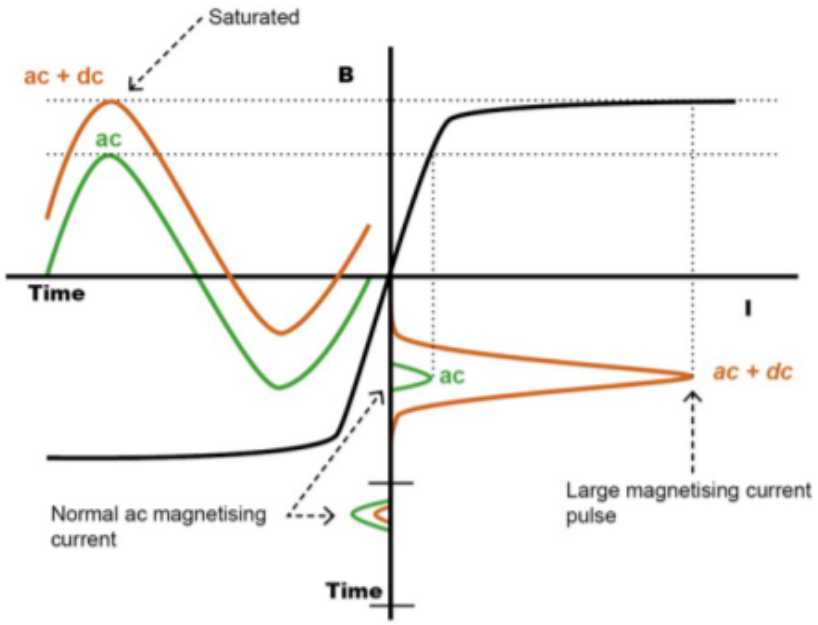

Figure 1.4: Magnetizing current waveform under with and without GIC [3]

During those half-cycles, the peaks of exciting current keep increasing and contain DC, fundamental, and even and odd harmonic components. The DC component of this current drops a voltage across the system resistance. This is subtracted from the DC voltage applied across the transformer magnetizing inductance. Thus, the rate of increase of the flux offset starts to decrease until the voltage drop across the system resistance equals the DC voltage applied, thus, completely negating it [4], as can be seen in Fig. 1.5.

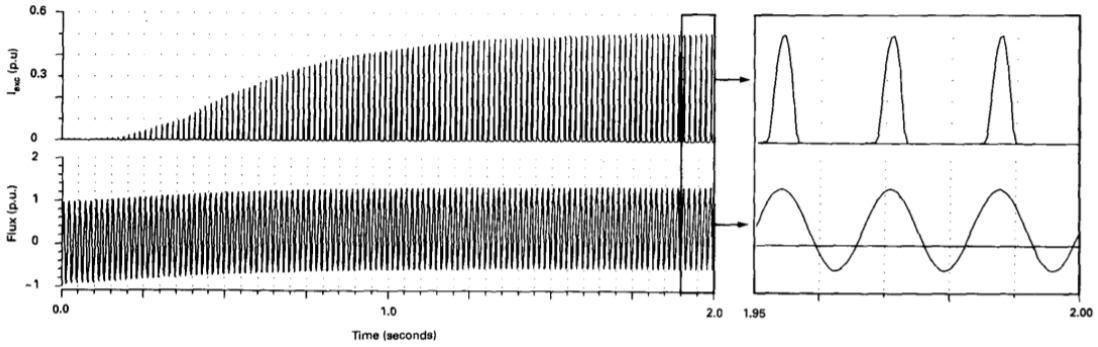

Figure 1.5: Magnetizing current and flux density waveforms of a nonlinear inductor model with DC voltage superimposed [4]

The above discussed case can be elucidated with the help of an equation [6]. For a transformer under no-load condition subject to a DC voltage V_{DC} whose system DC resistance can be taken as R_{DC}, according to Faraday's Law, the increase in linkage flux can be described as:

$$\Delta\lambda = \int_0^t V_{DC} - R_{DC} I_{mag}(t) dt \tag{1.17}$$

A corresponding Magneto Motive Force (MMF) would be required to drive the increase in linkage flux, which would be supplied by the magnetizing current, I_{mag} through the windings. When operating in the linear region of the transformer, i.e. region of high permeability, the required amount of magnetizing current will be low but as the transformer is driven into saturation, i.e., region of low permeability, the amount required will be very high, that is seen as peaks in every other half-cycle. In the rest of the half-cycles, due to the DC offset in flux, the amount of magnetizing current required would be lesser than normal.

From the above equation, it can be inferred that in the absence of a DC system resistance, the flux in the system will fail to reach steady-state. But the presence of DC resistances in the system are inevitable which are present by way of transmission lines, windings, etc. This, then, allows the system flux and thus, the magnetizing current, to reach steady-state when the voltage drop across the DC system resistance equals that of the induced DC voltage. The DC current flowing at this moment, which can be calculated as the ratio of the DC voltage to the DC resistance is the magnitude of GIC in the system.

In order to emulate the presence of a GIC in the system, this thesis will make use of a DC voltage source in series with a resistance, whose ratio should give the magnitude of the GIC under study.

1.1.3 Dependence on Type of Core

The performance of a transformer under GIC stresses is also dependent on the type of its core and the availability and structure of the return paths for the flux. The part of the core around which the windings are wrapped around any part parallel to it is known as the wound limb and the part perpendicular to the limbs which completes the magnetic path is known as the yoke. Broadly, they are classified as shell-type and core-type transformers (refer Fig. 1.6). In core-type transformers, all the limbs are wound by windings and the flux produced by a winding in one limb returns through the other limbs. Shell-type transformers have cores with winding-less limbs besides wound limbs to provide for extra return for flux and also to reduce the height of transformer for easier transport [1].
The amount of magnetization is affected to a great extent by the chosen core design. It has been

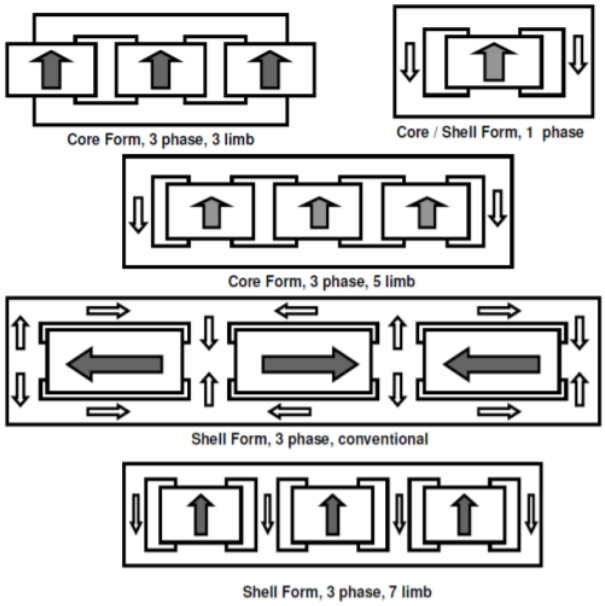

Figure 1.6: Different types of transformer core [5]

found that single-phase transformers, no matter their core design, tend to saturate in the presence of a GIC much more than their three-phase counterparts. This behaviour can be attributed to the fact that in the case of three-phase transformers, the effects of DC currents by way of DC flux in each phase is compensated by that in the other two phases through the wound limbs and yokes [6]. An exception to this case is the three-phase five-limb transformer, whose behaviour under GIC is similar to that of a single-phase transformer due to the presence of the return limbs.

This difference in behaviour can be further explained with the flow of zero sequence and positive sequence fluxes in the cores [6]. In single-phase transformers, the flow of both the sequence fluxes are along the same path, and since the reluctance of zero sequence path is very low, this can lead to easy saturation of the core. Whereas, in three-phase transformers, the two sequence fluxes flow through different paths, with the zero sequence flux taking the route in air, which has very high reluctance, and results in the core only saturating at very high magnitudes of magnetizing current. In three-phase five-limb transformers, though the paths taken by the positive and zero sequence fluxes are different, they are closed by the core like in single-phase transformers, implying they saturate at low magnitudes of GIC.

As a first step to understanding transformers under GIC through modelling and for the sake of simplicity of testing out a new modelling method, this thesis limits itself to exploring the effects of DC saturation within the scope of a single-phase transformer.

The effects of saturation in the core can be observed through ways such as uneven distribution of flux through the core with the highest flux density in middle of the main core limb and waning towards the ends of the limb into the yoke and the side limbs. This is possibly due to the reinforcement of the linkage flux by stray flux due to the increased current carrying windings [10]. This effect will also be observed in this thesis in the following sections.

1.2 LITERATURE REVIEW AND MOTIVATION

In research the ill-effects of GICs on transformers have given risen to making a numerical model that is as representative of the electro-magnetic (EM) behaviour of the transformer under GICs as possible without resulting in a computation heavy model, in terms of both space and time. So far, in literature and in practice, the numerical models proposed and used have predominantly been Magnetic Equivalent Models (MEM) which use lumped parameters and yields approximate results. The magnetic equivalent circuit is drawn by drawing analogies between the principles and elements of magnetic and electric circuits. This is then coupled with an external electrical circuit. This enables proper representation of winding and core topology, its nonlinearities and leakage fluxes[11][12][13]. MEMs sometimes also exploit the duality between electric and magnetic circuits to come up with an equivalent electric circuit which is then connected to the external electrical circuit[14][15]. The following table 1.1 would give an idea behind MEM.

Magnetic equivalent circuit	Electrical equivalent circuit
Reluctance	Inductor
Non-linear reluctance	Non-linear inductor
MMF	Two-port ideal transformer
Series connections	Parallel connections
Node	Mesh/loop
Mesh/loop	Node

Table 1.1: Duality between magnetic and electrical equivalent circuits

MEM is favoured over the next popular modelling method of Finite Element Modelling (FEM) due to their reduced computation time when observing the same behaviour. In FEM, governing Partial Differential Equations (PDEs) are solved over a problem domain using ordinary differential equations, where the domain is discretized and the solution is obtained by integrating the PDEs over the domain using methods such as Euler's, Runge-Kutta's, etc [16]. Since FEM computes over a finite number of elements spanning the geometry of the transformer, it yields detailed results at the cost of high computation time.

While research is being conducted to make MEM as accurate as possible, not much research has been done to reduce the computation load of FEM without using supercomputers [17]. As can be understood from the theory discussed in the previous sections, transformers when subject to GICs exhibit transient behaviour, i.e., take a few seconds to reach steady-state. Added to this, the dimensions of power transformers being in meters, it can cost hours of computation time before an FEM model is able to study their steady-state behaviour. Since this issue hasn't been addressed as such in literature, the main objective of thesis will be to try to reduce said computation time while using FEM for modelling the electromagnetic behaviour of transformers under GIC. Once achieving that, the next objective would be to conduct an electromagnetic study by way of winding loss calculation due to induced eddy currents in them.

1.3 STRUCTURE OF THESIS

An overview of how the thesis is structured is given below:

- *Chapter 1* provides background information on the principles of transformers, about geomagnetically induced currents, and their effects on power transformers.
- *Chapter 2* provides details on how the preliminary model of the transformer is built in the FEM software before it is modified for the timesaving method that will be discussed in Chapter 5.
- *Chapter 3* will expound on the results of electromagnetic study obtained for a few test cases run on the preliminary model built in Chapter 2 that will validate the FEM model.
- *Chapter 4* discusses how losses due to eddy currents in the transformer windings can be calculated when they are subject to GIC, using the model built in Chapter 2.
- *Chapter 5* proposes a way to reduce the computation load of the numerical modelling of transformers by transferring the load of computing the transient portion of the phenomena from FEM to a magnetic equivalent circuit constructed in MATLAB Simulink. The results from this modelling method is validated against that of the model built in Chapter 2.
- *Chapter 6* provides the conclusion to this thesis and suggest future scope for work.

2 MODELLING USING FEM

The transformer under study is a step-down auto transformer rated 280 MVA 500/230 kV manufactured by Royal Smit Transformers for Dominion Energy. Tests - both simulation and experimental - with and without GIC, have been conducted on the transformer by Royal Smit Transformers, previously. The simulation tests however solely utilized a Reluctance Based Model with lumped parameters. This chapter will show how to utilize Finite Element Modelling as a tool to run the simulation tests. Though FEM can be computation intensive, it provides greater detail into the behaviour of transformer. Thus, the goal of this chapter is to develop a FEM model that is least computation heavy while remaining as accurate as possible. Accuracy of the results from the FEM model is verified against that of the factory measurements and its effectiveness is compared against that of their reluctance model results.

2.1 BUILDING FEM MODEL

The details that went into building the simulation model in COMSOL is elucidated in this section.

2.1.1 Geometry

The development of the FEM model begins with building the geometry. The transformer is a bank of three single-phase auto-transformers. Only one of them will be analysed. Each has a two-legged core with two wound limbs as shown in Fig. 2.1. Of them, only one wound limb will be simulated. To ease the load on computation, a 2D-axisymmetric model of the wound limb cut in half along the line of symmetry perpendicular to the rotational axis of symmetry, is implemented in COMSOL as shown in Fig. 2.2.

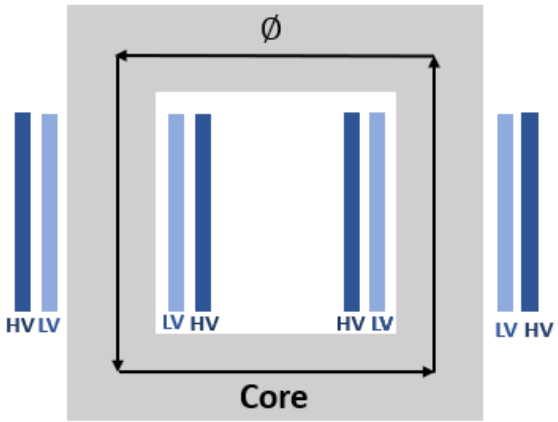

Figure 2.1: Flow of flux through a two-limb single-phase transformer [6]

The two core-legs of the real-life transformer ensures the flow of flux produced by both the sets of windings is along a closed magnetic path as shown in Fig. 2.1. Thus, simulating just one of the wound limb implies a return path for the flux must be given, for the purpose of which unwound return limbs are implemented. But, in a 2D-axisymmetric model, if the geometry of the return limbs is given the same thickness as that of the wound limb it would lead to an increasing cross-section for the flux to flow away from the rotational axis of symmetry, as the given 2D planar geometry rotates.

To resolve this, the thickness of the upper and lower return limbs vary according to Eq. 2.2 depending on its distance from the rotational axis of symmetry. The thickness of the side return limb is determined according to Eq. 2.3.

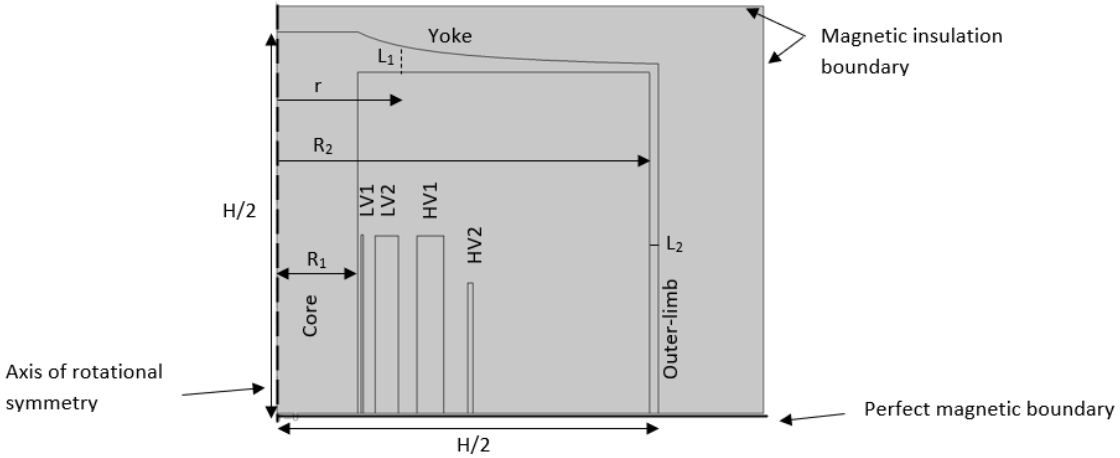

Figure 2.2: Equivalent 2D axisymmetric geometry of the transformer

If the yoke in the revolved geometry is to have the same cross-section as that of the core limb at any point r from the axis of rotational symmetry,

$$2\pi r L_1(r) = \pi R_2. \tag{2.1}$$

Thus, the thickness L1 of the yoke decreases from position $r = R_1$, as

$$L_1(r) = \frac{R_1^2}{2r} \tag{2.2}$$

The outer-limb thickness is then given by

$$L_2 = -R_2 - \sqrt{R_2^2 + R_1^2} \tag{2.3}$$

where

$$R_2 = \sqrt{(H/2)^2 - R_1^2}. \tag{2.4}$$

The windings are approximated as a homogenized coil whose turn and material specifications will be specified in the magnetic field physics, thus they take the shape of a rectangle covering their cross-section in the 2D-axisymmetric geometry instead of individually chalking out the windings which would again increase the number of mesh elements and in turn the computation time. The enclosing environment is provided by a rectangle with its sides as far away from each limb as in the real-case scenario to allow enough space for flow of leakage flux as in the real case. Once the geometry is built, all enclosed spaces are referred to as domains while their edges are referred to as boundaries.

2.1.2 Materials

The material of all the domains are by default set to that of air, by COMSOL. The additional materials and their properties specified for the domains individually, thus, overwrites the properties of air.

The only thing altered under the materials node of the model (2.3) is adding a Soft Iron (Lossless) material and overwriting the values of BH Curve attribute present under it. These values are specified as a table in an interpolation function. Within the settings of the interpolation function, the interpolation and extrapolation are set to Linear to ensure gradually monotonically increasing traversal of the solver across the curve, since setting the extrapolation to Constant resulted in crashing of the solver as it tried to take smaller steps after reaching saturation. The settings for the material for the windings will be later set in Magnetic Fields Physics interface that will be discussed later in this chapter. These settings will overwrite the specifications set in the Materials node.

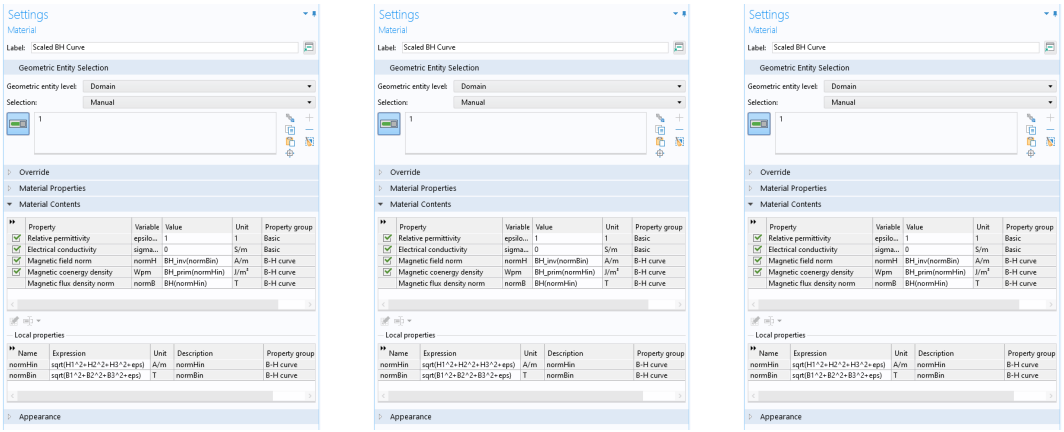

Figure 2.3: Material settings

Lamination Factor

The B (magnetic field intensity) values entered in the table in this node are however modified. This is done to take into account the fact that the flow of flux through the core is affected by the presence of laminations in the core. Thin sheets of few tens of millimeters thickness of a material with the desired ferromagnetic properties are stacked, with the sheets placed in a direction parallel to the flow of induced flux. This is done to avoid the induction of eddy currents and its associated heating losses within the core. The stacking of these thin sheets, in turn, reduce the effective area of cross-section of the core, which in turn reduces the area through which the flux flows. The cross-section of the core would thus look as illustrated below in Fig. 2.4:

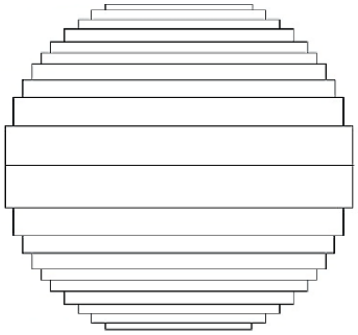

Figure 2.4: Top view of a limb of a laminated core [7]

The stacking/lamination factor for the core is given as the ratio of the effective cross-sectional area of the core to its total geometric cross-section. For the transformer under study, the lamination factor is 0.9. Thus, the values of B (magnetic induction, i.e. flux per unit area) in the BH curve values recorded by the company for the transformer under study, is divided by the lamination factor to imitate the effective cross-section instead of simulating thin laminations which can be highly computation intensive in a FEM software as it leads to increase in the number of mesh elements. The modified BH-Curve used thus, looked as shown in 2.5.

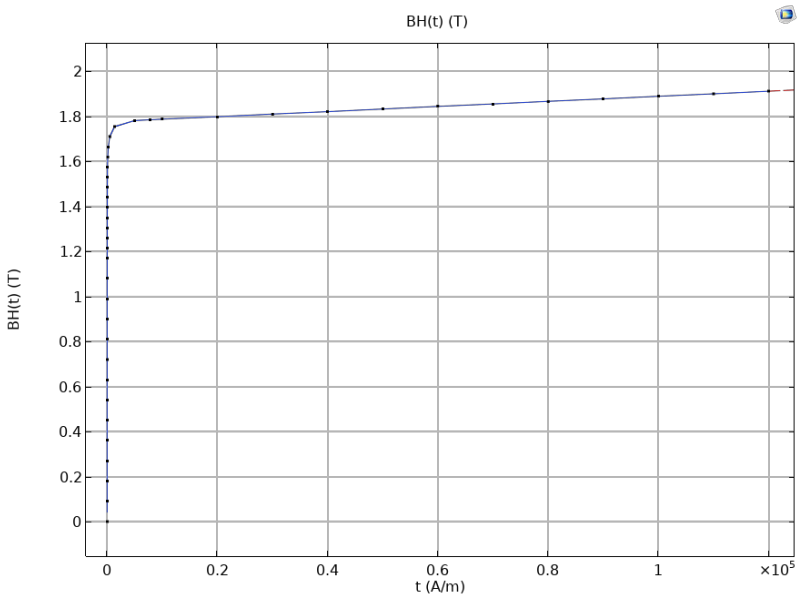

Figure 2.5: BH curve of the core accommodated for the lamination factor

2.1.3 Physics Interfaces Applied

The magnetic fields (mf) physics and electric circuit (cir) physics have been applied to the model to achieve the desired physics behaviour.

Magnetic field physics interface

Under the mf physics, the default settings have been left untouched. While, additionally, the following are applied to the core and windings domains:

- Ampere's law domain condition is applied to the transformer's core domain. Under the condition's settings, the constitutive relation is chosen as B-H curve since that is the option

that refers to the B-H curve mentioned in the material properties while the other options ignore it and consider a constant permeability. Their governing equations are shown below:

$$\vec{E} = -\frac{\partial \vec{A}}{\partial t} \tag{2.5}$$

$$\nabla \times \vec{H} = \vec{J} \tag{2.6}$$

$$\vec{B} = \nabla \times \vec{A} \tag{2.7}$$

$$\vec{J} = \sigma \vec{E} \tag{2.8}$$

- A coil domain condition is applied to each of the windings. Under the condition's settings for each winding, the conductor model is chosen as homogonized multi-turn conductor which opens a section where the number of turns, winding conductivity, and effective turn cross-section are specified. The coil-excitation is chosen as Current (circuit) as the current flowing through the circuit that will be specified under the Electric Circuit physics determines the excitation of the coil. Their governing equations in COMSOL are as follows:

$$\vec{J_e} = \frac{N I_{cir}}{A} \vec{e}_{coil} \tag{2.9}$$

- Perfect magnetic conductor boundary condition is applied to the horizontal line of symmetry cutting the transformer in half. This boundary condition ensures that current can only flow parallel to the boundary which agrees with the desired behaviour of the current through the windings. It also ensures the flow of magnetic flux is only permissible perpendicular to the boundary condition which again bodes well with the desired core performance. The equations governing them are:

$$\vec{n} \times \vec{H} = 0 \tag{2.10}$$

Electric circuit physics interface

In this physics interface each element added under it is connected by specifying their positive and negative terminals in the circuit of desire under each element's settings. The following elements are the ones of relevance to this thesis, and their inclusion and connection between each will be mentioned as per the test case.

- An External I vs. U node is added for each winding where their source of voltage is chosen as the coil in the Magnetic Fields physics interface corresponding to that winding as shown in Fig. 2.6.
- Voltage source elements are added to the circuit when AC and/or DC voltage sources are required. The desired type of voltage source is thus mentioned under Source Type. For AC voltage, the Source Type is chosen as Sine Source where its amplitude, frequency and phase are mentioned. Sine Source is chosen instead of AC-Source since the latter is only applicable in the frequency domain while the former is only applicable in the time domain. Under the setting of Sine Source, its amplitude, frequency and phase are mentioned. The amplitude is varied according to the test case. The frequency remains the same at the rated

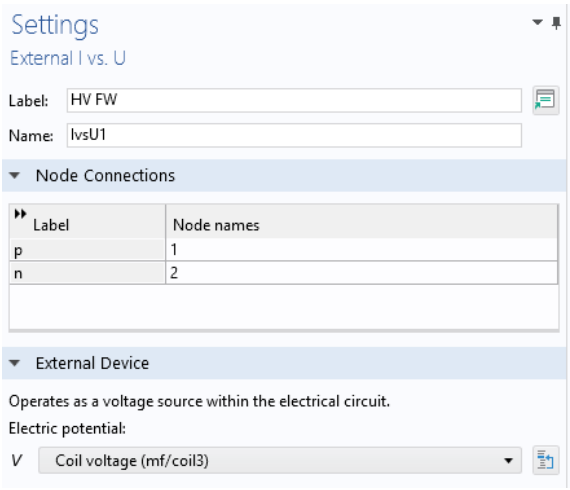

Figure 2.6: External I vs. U node settings

frequency of the transformer, at 60 Hz. The phase also remains the same at $\frac{\pi}{2}$ radians (refer Fig. 2.7)

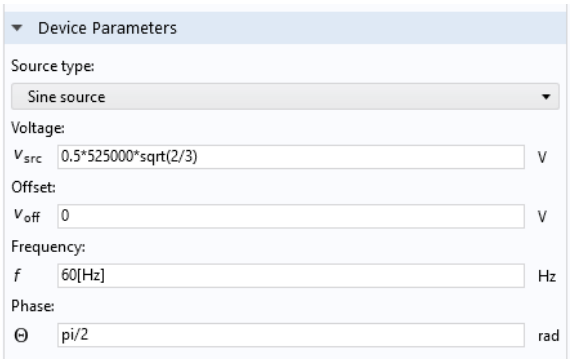

Figure 2.7: AC voltage source settings

Inrush currents: The phase of the sine-source is specified as $\frac{\pi}{2}$ radians to avoid inrush currents which occur if the transformer is switched on at the zero-crossing of the applied voltage. Since the induced flux will be the integral of the applied voltage, the value of flux at $\frac{\pi}{2}$ radians after the voltage is started from zero will be twice as much as the peak steady-state flux which is also the rated flux above which the transformer is pushed into saturation. Above the rated flux value, the current that needs to be drawn by the transformer to produce the rest of the flux peaks to a high magnitude owing to the non-linearity of the B-H characteristics. Inrush currents are transient where the peaks decay and reach steady-state value at a time corresponding to the time constant of the circuit determined by the ratio of inductive impedance to its resistive impedance, which might take a few seconds. Since the FEM model is computation heavy owing to the dimensions of the transformer and the number of mesh elements to obtain smooth distribution plots, the rate of solving this simulation will be slow and it is best to avoid situations where the GIC needs to be applied after waiting for a couple of seconds for the inrush currents to decay.

For DC source, the source type is chosen as DC Source and its amplitude is mentioned. Since the DC source in series with a resistance is applied to simulate a GIC source, the DC source is given with a step voltage. This is achieved by mentioning the desired voltage

amplitude multiplied by a step function defined at the desired time with the desired slope. The step function can be defined under Global Definitions in COMSOL or under Definitions present under the Component this model is being built in depending on the desired scope of the function.

- Resistances are added for the purposes of acting as the GIC resistance which when in series with the GIC DC source produce the required GIC current, as well as to as a load.
- Current source is used in a test case when GIC needs to be supplied to the secondary electrically isolated from the primary. Current source ensures there is no voltage drop across it assuming infinite resistance whereas if the GIC were to be simulated as a DC source with a resistance in this case would lead to the resistance acting as a load.

2.1.4 Mesh

A default mesh of triangles is applied to all of the domains as shown in Fig. 2.8. The maximum size of the mesh elements are however modified for the various domains by applying a value of 70 mm maximum element size for all of the domains and over-writing it by adding a Size attribute under a Free Triangular subnode to the Mesh node. Under the Size attribute, the domains of only the transformer core and windings are selected and applied a maximum element size of 20 mm. These values are mentioned to ensure the distribution plots obtained aren't too coarse nor inaccurate while also not being computation intense. The mesh for the core and the windings is much finer than that of the rest because their study is of importance to this thesis analysing the losses within them and their behaviour.

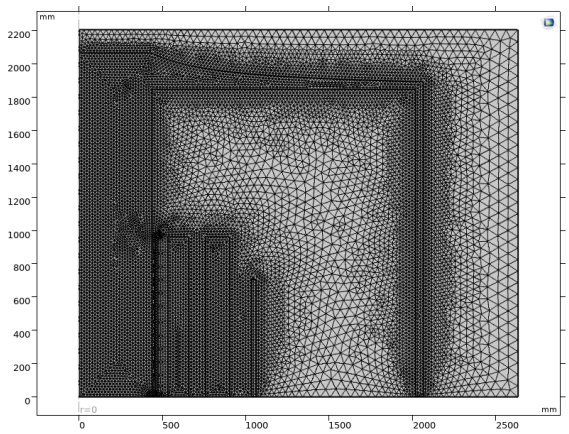

Figure 2.8: Mesh defined for the 2D equivalent FEM model

2.1.5 Study

GIC is a transient phenomenon that takes some time to reach steady-state. Thus, it prompts the use of a Time-Dependent Study in COMSOL so that the GIC behaviour needs to be observed over time. A time dependent solver subnode is added to the time dependent study by selecting Show Default Solver from the Study toolbar

The following changes have been implemented to the default time dependent solver settings after several trials and convergence issues faced. Each setting change and their reason have been elucidated below.

- Under the General section of Time Dependent Solver subnode, User Defined is selected to from the list against Defined by Study Step. In the Times the time steps to be associated

with the outputs at each step is specified, even though the simulation will run from the beginning irrespective of the starting output time mentioned. It's usually specified as range(start output time, step size, end output time). The Relative Tolerance field is used to specify the number that will control the relative error of each time step. It is decreased from its default value to a tighter value of 0.001 has been found to be optimal case for simulating normal and GIC cases, achieving fast rate of run time without compensating quality of output.

- Under the Time Stepping section of Time Dependent solver subnode, the time-stepping method is chosen as BDF. From the Steps Taken By Solver list that appears, Free is chosen. This option allows the time-stepping method to choose the time steps freely and overrides the time steps mentioned in the general section. Thus, from the Maximum Step Constraint list, Constant is chosen and a value of 0.0001s is entered in the Maximum step field that appears. This implies the solver is allowed to take step sizes freely upto the value of 0.0001s. This is done to ensure the step sizes taken by the solver are not too large when the computation becomes intensive, which can be analyzed by looking at the Convergence Plot appearing as a separate window when running a simulation.

  For time-dependent solver, the convergence plot shows the reciprocal of time step size versus the time step. If the convergence plot shows decreasing values, it implies it is taking very large step sizes to solve trying to reduce the intensity of computation leading to inaccurate results and convergence issues.

  Convergence issues were faced (as shown in Fig. 2.9) especially right before the magnetizing current of the transformer with a GIC tried to reach its steady-state since the solver tried to take large time steps when traversing the saturation region of the BH-Curve to its far end. This issue was solved by explicitly specifying a Maximum Step Constraint.

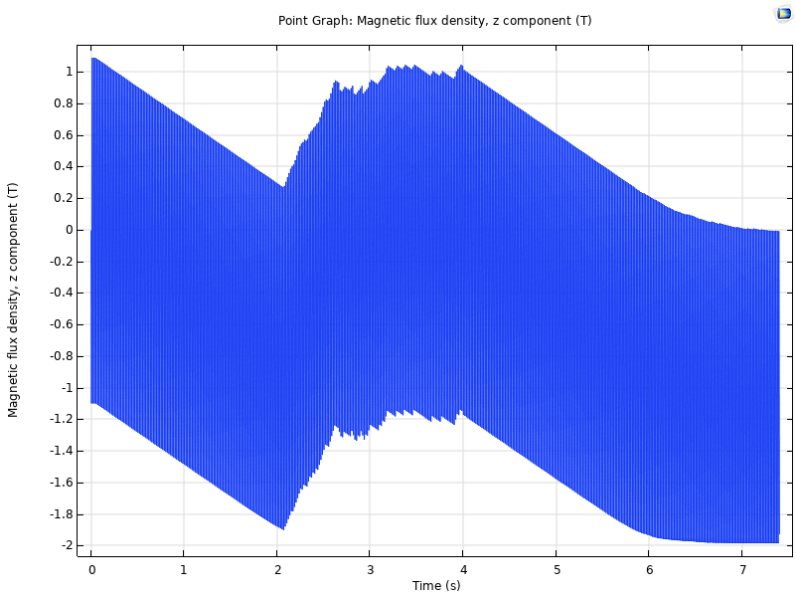

Figure 2.9: Convergence issue faced

- Under Dependent Variables node, in the Scaling section, Method is chosen as Automatic which lets the solver choose the peak values for the different dependent variables it solves for. While in the Residual Scaling section the method is chosen as Manual and a value of 0.001 is entered in the Scale field that appears. Residual scaling determines the error

termination and the choosing 0.001 over the default value of 1 helped solve convergence issues faced.

- Under the Direct node the linear system solver is chosen as Pardiso was the only solver from the options that didn't lead to convergence issues when running GIC simulations.
- Under the Fully Coupled node, in its settings window, under the Method and Termination section, the Nonlinear method is chosen as Constant (Newton) with a damping factor of 1 and from the Jacobian Update list, On Every Iteration is chosen. In the maximum number of iterations, 25 is entered. This is done to ensure the solver is iteration dependent instead of on relative error which makes the simulation more robust. The number of iterations is increased from the default value to ensure increased accuracy. Decreasing the Tolerance factor from the default value of 0.1 to 0.01 decreased the computation time as the solver took steps more smoothly.

After the above modifications to the default time dependent study step and solver settings are done, the model is computed.

3 TESTING THE FEM MODEL

In this chapter, the FEM model built in the previous chapter is tested for various cases and validated.

3.1 NO-LOAD BEHAVIOUR WITHOUT GIC

In the factory measurements that were taken for no-load case of the auto transformer, voltage was applied only to the LV1 winding, as shown in Fig. 3.1. The applied voltage ranged from 58.73% to 114.52% of the rated voltage for the LV1 winding.

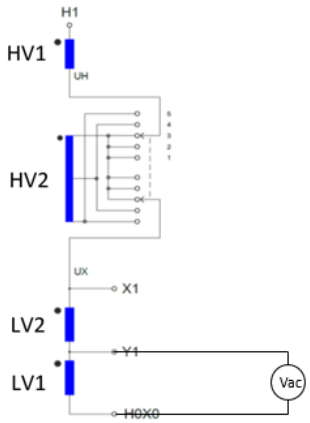

Figure 3.1: Circuit connections to verify no-load behaviour without GIC

In COMSOL, the circuit connections are specified in the Electric Circuit interface as per the above figure. Since the software doesn't allow any open nodes to be present, a volt meter (imitating infinite resistance) is connected across the windings other than the LV1 windings to close the circuit. The amplitude of the sine-source supplied to LV1 is given as a product of its rated voltage and a variable specifying the desired percentage. This variable is defined under Global Definitions.

Under the Time Dependent study, a Parametric Sweep step node is added. There, the variable to sweep over is chosen and the range of values are specified in the field next to it as shown in Fig. **??**. The model is then computed from 0 to 3 seconds.

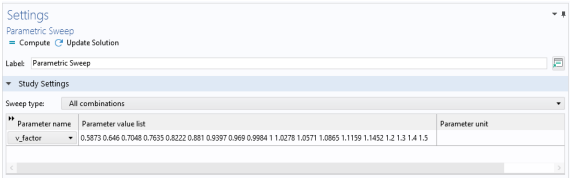

Figure 3.2: Parametric sweep settings

After it is done computing, in the Results node, a 1D Plot Group is added under which a Global graph is added. The dataset is chosen as the parametric sweep solutions. The magnetizing current through the LV1 winding and the voltage across it, is plotted for all of the time steps and for all of the percentages of rated voltages applied. In order to post process these results and compare them against the factory measurements, they are transported to MATLAB. In the Export subnode under Results, a Plot subnode is added. This indicates the data in a plot needs to be exported. In the Plot export's settings window, the dataset is chosen as that of the Global graph under the 1D plot group. The format for it to be exported as, its file destination and the type of separation are specified. The plot containing the results for the parametric sweep of the varying voltages is exported as a comma separated text file. This is opened in MATLAB and post-processed. In MATLAB, the average value of the absolute values of the current and voltage plots obtained as well as the factory measurements are plotted together against the magnetic induction at each voltage level. This comparison can be seen in Fig. 3.3.

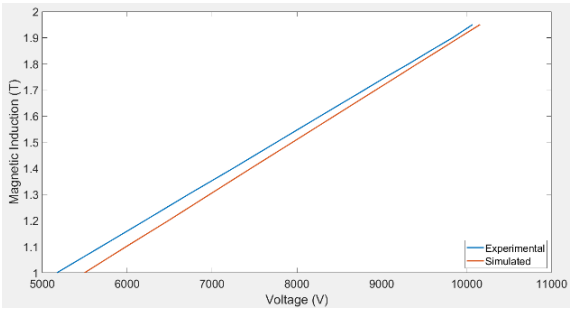

(a) Voltage verification

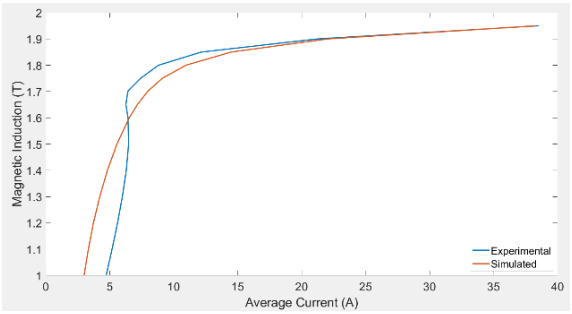

(b) Current verification

Figure 3.3: Verification of FEM model under no-load no-GIC condition

As can be seen, the simulated values are in close agreement with the factory measurement values.

As an additional step of verification of the COMSOL model, the peak magnetic induction of the transformer for this set up at various percentages of the rated voltage is found. Regardless of the set of windings energized, at rated voltage supply of that set of windings the core will have rated flux density.

Percentage of rate voltage	100	115.9	120
Peak magnetic induction from factory measurement (T)	1.7027	1.9	2.043
Peak magnetic induction from COMSOL (T)	1.7	1.9	2.02

Table 3.1: Verification of no-load no-gic magnetic induction measurements

The magnetic induction is measured at the center of the core. For this, a Cut Point should be added under the Dataset attribute of Results subnode and the coordinates of the desired point is mentioned. A Point Graph is added under a 1D Plot Group and choosing the CutPoint as

the dataset the magnetic field intensity is plotted. This plot for the different voltage levels are shown in Fig. In Table 1, the factory measurement values of magnetic induction in the core at different percentages of the rated voltage are given, beside which the magnetic induction peak obtained via COMSOL is recorded as well. Again, they are in close agreement with each other, thus verifying the no-load no-GIC behaviour of the auto-transformer model in COMSOL.

For 1, 1.159, 1.2, 1.3, 1.4, 1.5 times the rated voltage U_r, the magnetizing current plots and magnetic induction plots in the core over time have been shown in Table 3.2. This range of voltages have been chosen to observe how saturation is reached and how it affects the magnetizing current as well as the magnetic flux density.
As can be seen with increasing supply voltage, the current waveform becomes peaky in both the half-cycles, following the shape of waveform predicted in the theory explained in section 1 for transformer approaching AC saturation. The magnetizing current peak is also seen to increase exponentially with a slight increase in the peak magnetic induction. It can be seen that saturation occurs in both the half-cycles leading to the presence of odd harmonics as explained before.

The FFT analysis on the magnetizing current in COMSOL is carried out by choosing Frequency Spectrum under x-axis Data section of the 1D Global Graph settings. To observe the RMS magnitude of current for each frequency component the scale check-box is ticked. The obtained graph is shown in Fig. 3.4

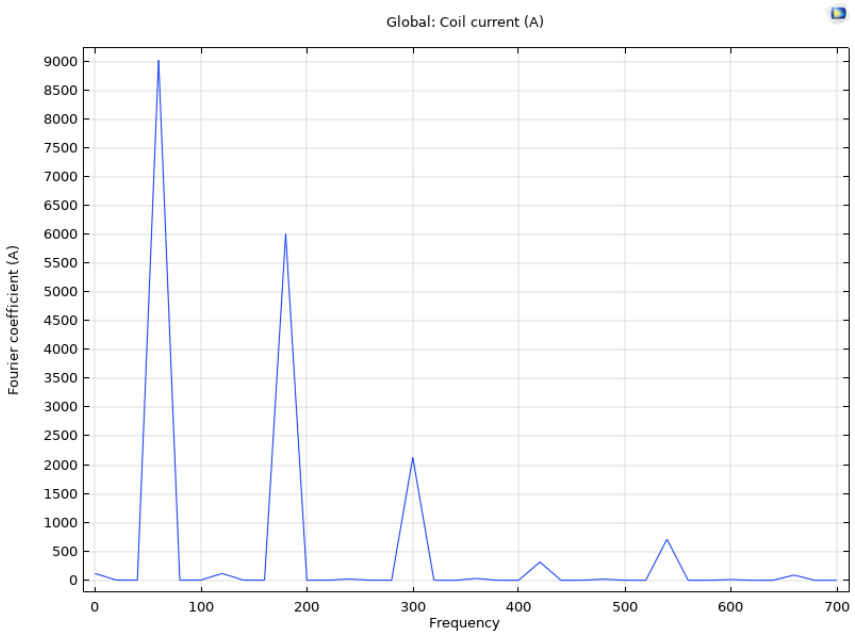

Figure 3.4: Harmonics distribution of magnetizing current under no-GIC

The distribution of the magnetic flux density in the core and the windings is also observed at the same voltage levels as above. To get the magnetic flux density distribution a 2D Plot Group is added under which a surface plot is added.

	Magnetizing current over time	Magnetic induction in the core over time
1 U_r	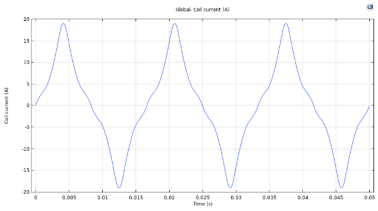	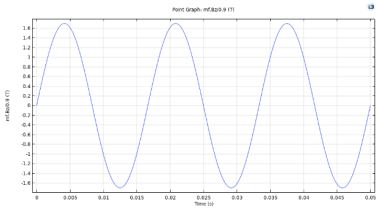
1.159 U_r	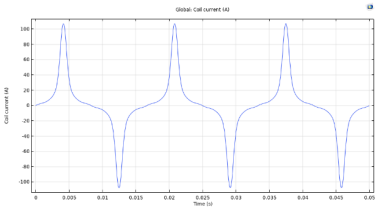	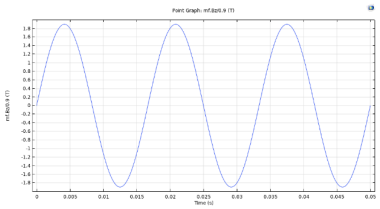
1.2 U_r	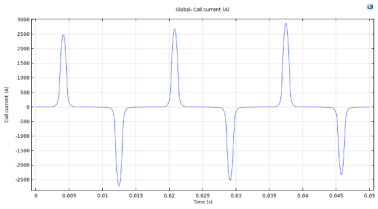	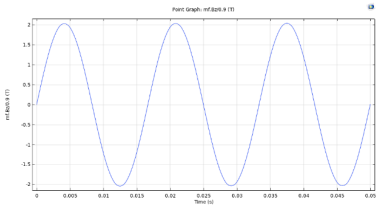
1.3 U_r	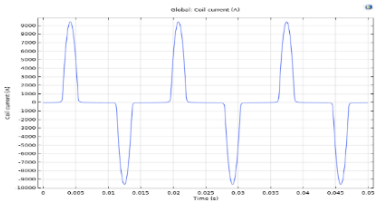	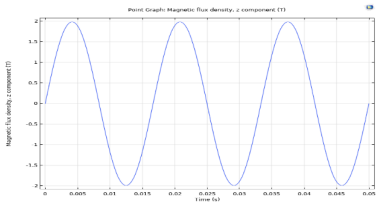
1.4 U_r	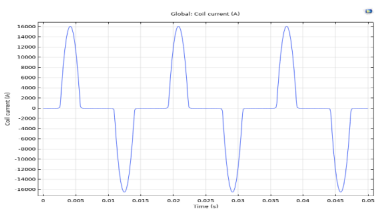	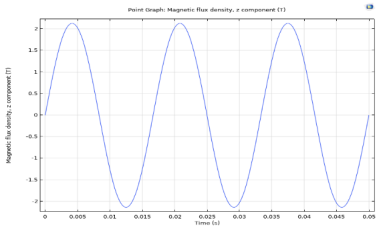
1.5 U_r	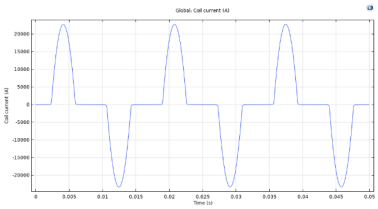	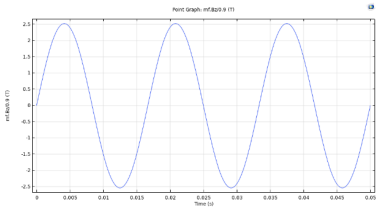

Table 3.2: Waveforms for no-load condition of the transformer without GIC

To obtain the distribution of magnetic flux density in the windings, create a selection under Time-dependent study feature present beneath the Dataset subnode of the Results node. In the selection window settings, choose only the winding domains. Then plot the surface plot for magnetic flux density again and it will be plotted only for the windings as shown. At the time of peak of the magnetic flux density, its surface distribution plot is plotted as shown in Table 3.3. As can be noted, as the transformer reaches saturation, the core leg begins to saturate in the middle more than the rest of it. And as saturation is approached (from 1,2 Ur onwards, the flux density peak increase greatly and is concentrated for the most part in LV1).

In addition, magnetic flux lines plots for the same voltage levels were plotted to analyse their behaviour with increasing voltage as shown in Table 3.4. This was done by plotting a 2D contour plot for the expression r*mf.Aphi which is the product of radial distance from the rotational axis of symmetry and the magnetic vector potential which ultimately yields magnetic flux in Webers and when a contour plot of the same is plotted, we obtain magnetic equipotential surface with the magnetic flux lines. The same number of lines (25) are chosen to plot each of them for ease of comparison.

As can be noted with Table 3.4 as the transformer reaches saturation, the core leg begins to saturate in the middle more than the rest of it. And as saturation is approached (from 1,2 Ur onwards, the flux density peak increase greatly and is concentrated for the most part in LV1).

	In the core	In the windings
1 U_r	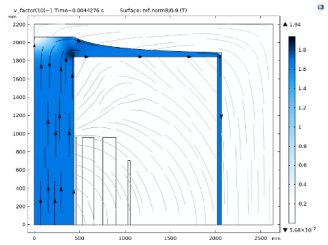	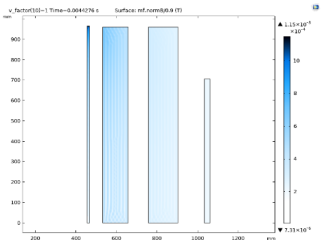
1.159 U_r	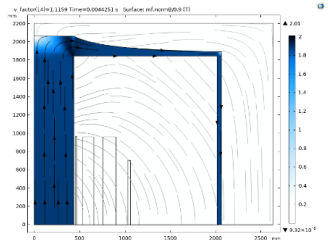	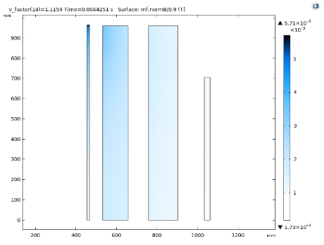
1.2 U_r	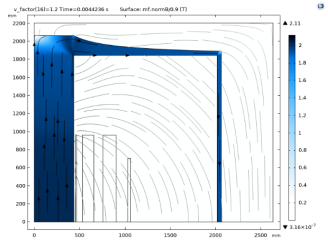	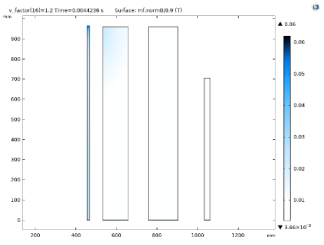
1.3 U_r	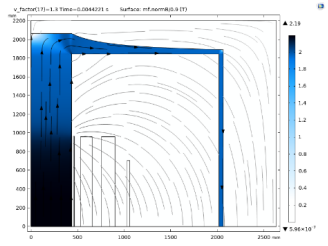	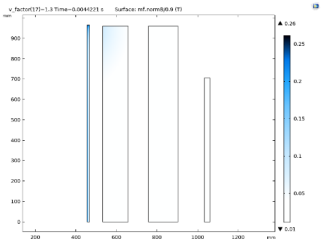
1.4 U_r	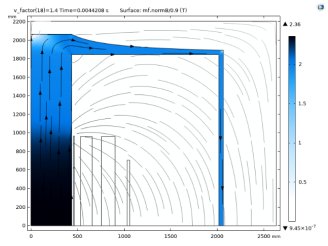	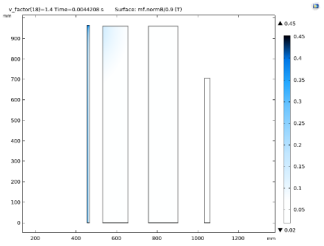
1.5 U_r	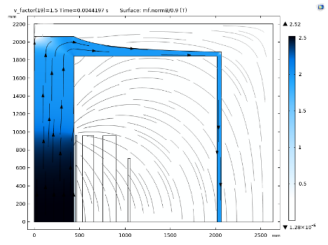	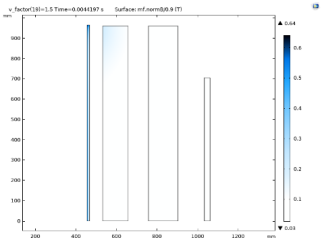

Table 3.3: Magnetic flux density surface plots at peak induction

	In the core	In the windings
1 U_r	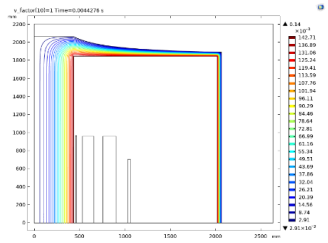	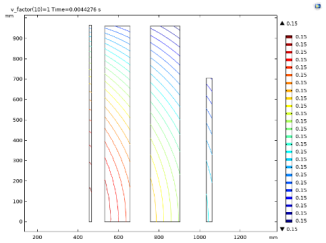
1.159 U_r	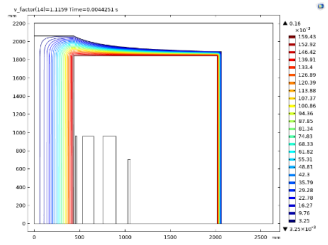	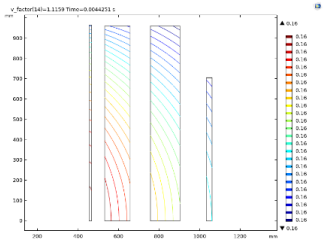
1.2 U_r	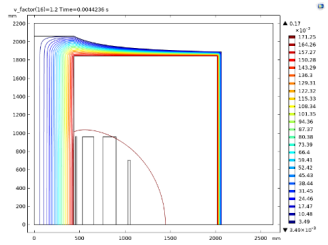	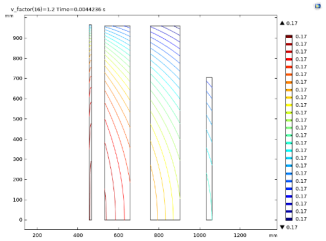
1.3 U_r	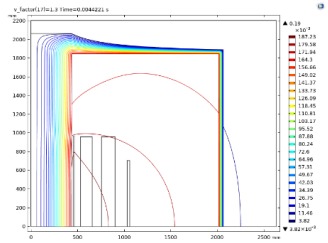	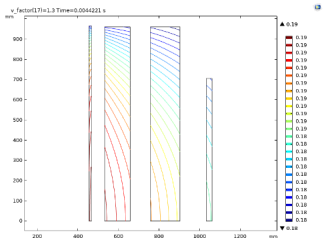
1.4 U_r	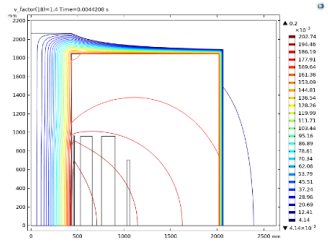	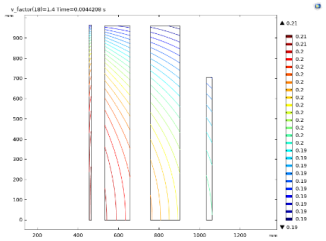
1.5 U_r	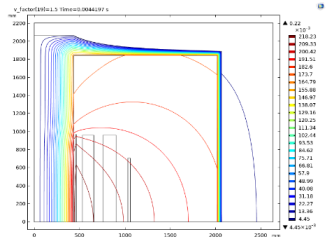	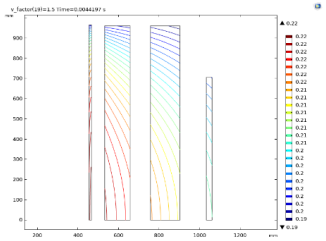

Table 3.4: Magnetic flux surface plots at peak induction

3.2 NO-LOAD BEHAVIOUR WITH GIC

To analyse the no-load behaviour of the auto-transformer under GIC, the following set-up shown in Fig. 3.5 has been implemented in COMSOL. The necessary connections between the elements were specified in the Electric Circuit physics interface. The following test-case was for a scenario were a GIC of 75A is injected into the primary of the auto-transformer with the help of a DC voltage source of 750V in series with a resistance of 10 . The rated AC voltage in series with this GIC source is supplied across the terminals of the primary.

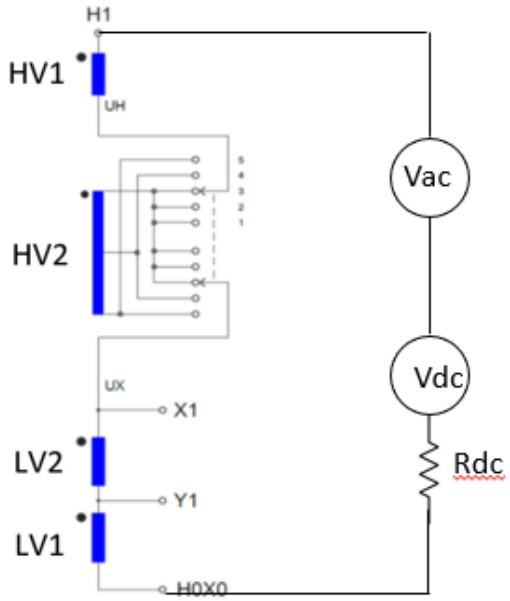

Figure 3.5: Circuit connections for transformer under no-load with GIC condition

The following magnetizing current graph was obtained. As can be observed, the shape of the waveform resembles that of the magnetizing current shown in Fig. as the above set-up is equivalent to powering an inductor with an AC voltage source and DC current source as discussed in section. It can be seen that the current reaches steady-state at around 1.5 seconds when the voltage drop across the resistance equals that of the DC voltage supplied as seen in Fig. 3.6.
Zooming into the current after reaching steady-state, peaks in half-cycles and reduced current in the other half-cycles due to DC saturation can be observed (3.7).
This type of a waveform implies the presence of even and odd harmonics as opposed to just odd harmonics as seen in the AC saturation case which is shown in 3.8.

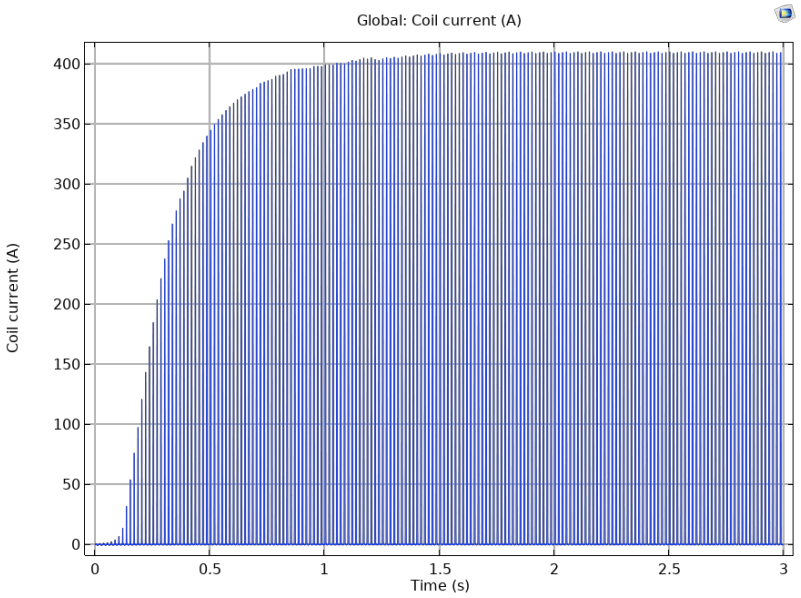

Figure 3.6: Magnetizing current waveform under no-load with GIC (75A) condition

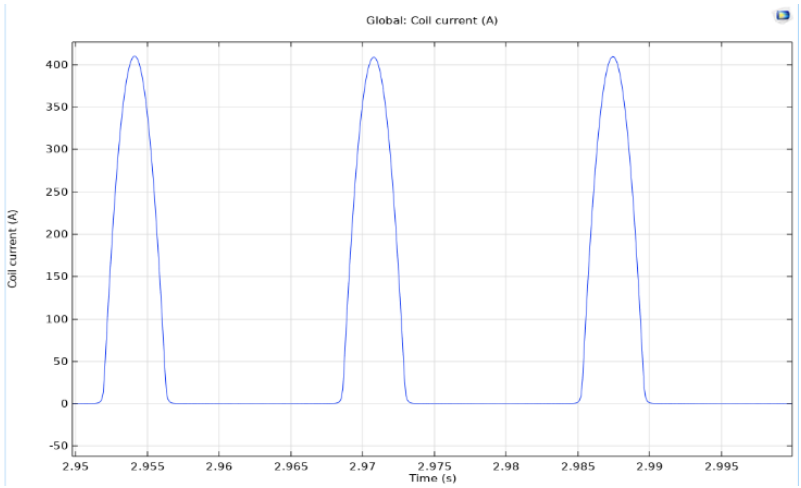

Figure 3.7: Magnetizing current waveform under no-load with GIC (75A) condition (zoomed in)

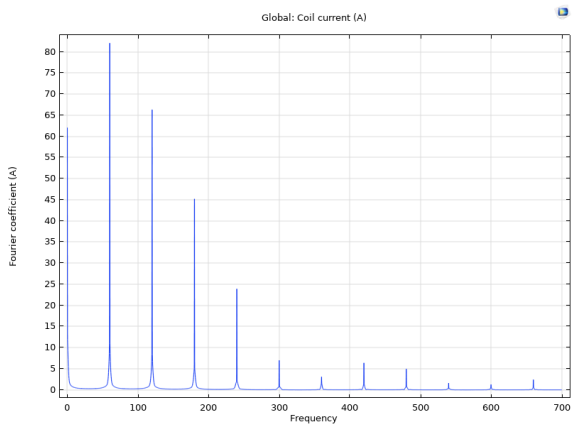

Figure 3.8: Magnetizing current harmonic distribution under no-load with GIC (75A) condition

The magnetic flux density graph over time for this test-case is shown in 3.9a. It appears to reach steady-state earlier than the magnetizing current but this can be attributed to the fact that once saturation is approached small increase in the magnetic induction value can lead to a very large increase in the magnetizing current value. Zooming in to three cycles of the steady-state magnetic flux density the flat-topping of the wave in half of each cycle can be seen indicating the presence of a DC off-set of the flux (Fig. 3.9b).

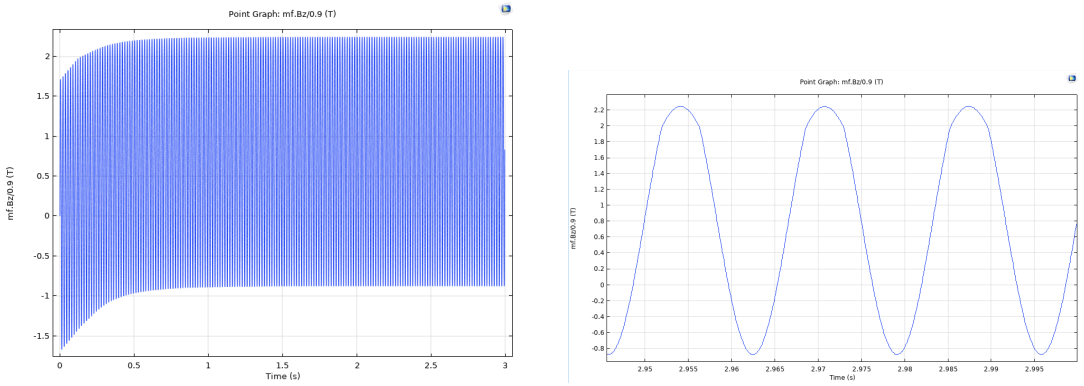

(a) Over entire run time **(b)** Over last 3 cycles

Figure 3.9: Magnetic flux density waveform in the core

The flux density distribution in the core and the windings are shown in Fig. 3.10.

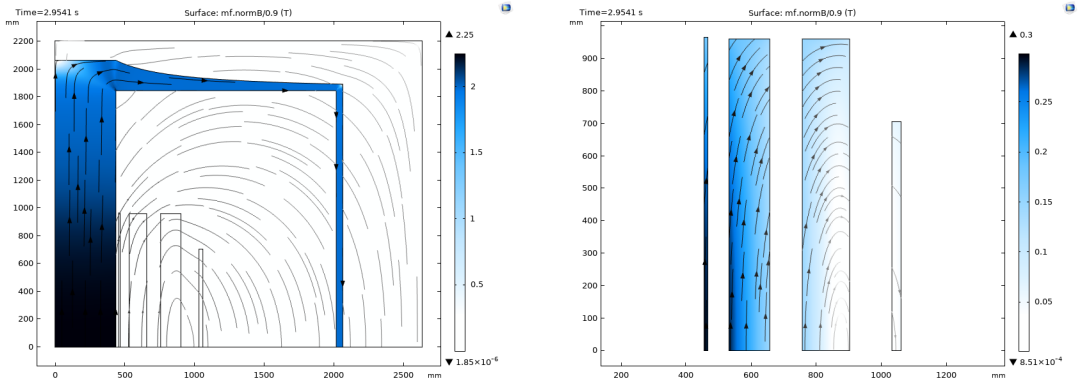

(a) In the core **(b)** In the windings

Figure 3.10: Surface magnetic flux density distribution

As can be observed from the above flux distribution plots, the core of the transformer under GIC behaves similar to AC over voltage saturation and shows extreme saturation in the middle of the core leg. But the distribution of the flux density in the windings differ greatly from that of any case without GIC. The high magnitudes of flux density is shared not just by LV1 as in the case without GIC but also by LV2 and to an extent by HV1 indicating higher risk of damage for LV2 and HV1 windings which are the windings of importance since most of the voltage is induced/dropped across them.

Thus, it becomes imperative to calculate the losses and the distribution of those losses within them to predict the extent of damage in the regions within the windings. This will be discussed in the next section.

4 EDDY CURRENT LOSSES IN THE WINDINGS

Losses in the windings can be due to inherent resistive losses due to the current through the windings or due to the eddy currents induced in them due to the leakage flux.

Resistive losses can be calculated as the product of the RMS current - which is the DC equivalent of the current through the windings - and their DC resistance.

$$P_DC = I^2R \tag{4.1}$$

The equivalent 2D axisymmetric model of the transformer considered in this thesis represents each set of windings as a rectangle covering its entire cross-section. The number of turns specified along with the conductivities of each set of windings is taken to be spread uniformly across their corresponding rectangles by the FEM software. Thus, the current density calculated by the software remains the same through the whole area of each set of windings. The winding losses calculated by the software would not then take into account the effect of eddy currents due to leakage flux and would only give the resistive winding losses. This will not be the case if each strand of the windings were to be modelled, whose behaviour would then be closer to reality. In that case, the losses given out by the software would be the sum of DC losses as well as the eddy current losses.

To avoid having to model each strand in order to calculate the winding eddy current losses, which can be computationally intensive, a way to calculate the winding eddy current loss from the equivalent model is proposed here using the expression for finding the eddy current losses in a rectangular strand of conductor proposed in [6]. The expression is derived by assuming that the magnetic field intensity remains the same through the cross-section of the conductor for both the axial and radial components of the field intensity. The expression then takes the axial and radial components of the peak magnetic field intensity in the middle of the conductor to be the average field intensity throughout the conductor and then calculates the respective eddy current loss components. The total eddy current loss of a winding set is then obtained by the simple summation of the axial and radial components of the loss, assuming that they are both perfectly orthogonal to each other.

Thus, each rectangle representing a set of windings in the equivalent model is divided into as many sections as possible to increase accuracy while ensuring it is not computationally heavy, by trying to make the dimensions of those sections as close to that of the strands of the real windings. The midpoints of these sections are then considered to measure the magnetic field intensity from the results of the FEM software as shown in Fig. 4.1. In COMSOL, these set of points for post processing the results can be obtained by choosing Results→ DatasetCut → Point 2D. In the setting window of Cut Point, choose to specify the points using an external file. The file should contain the coordinates of the points to measure the intensity from for each set of windings.

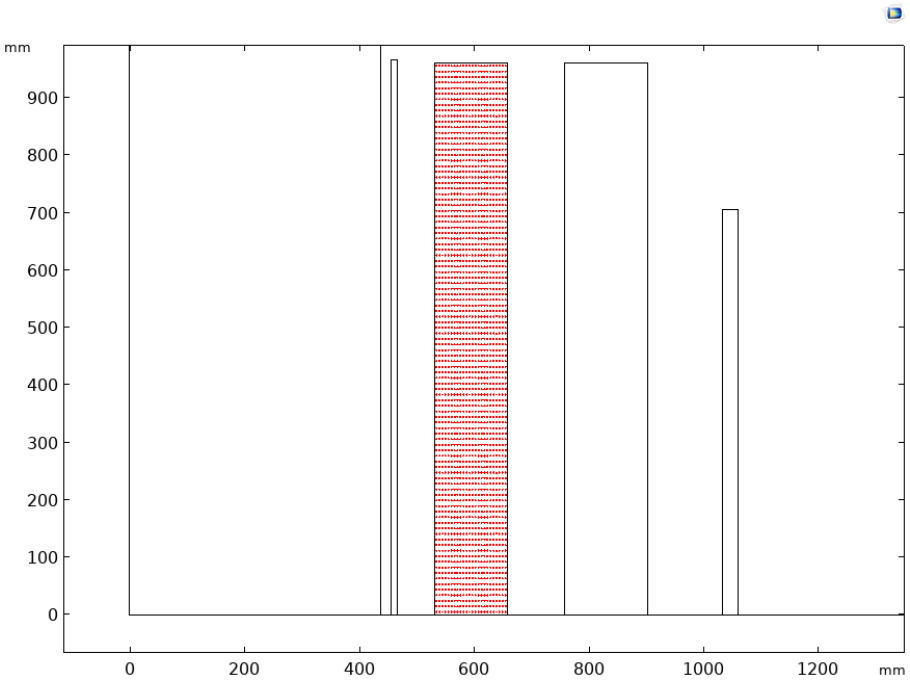

Figure 4.1: 2D cutpoints considered in COMSOL to extract H values from

If at each point a section representing the conductor with dimensions as shown below in Fig. 4.2 are considered to be placed in a magnetic field of peak intensity H_0, that can be resolved into its radial and axial components,

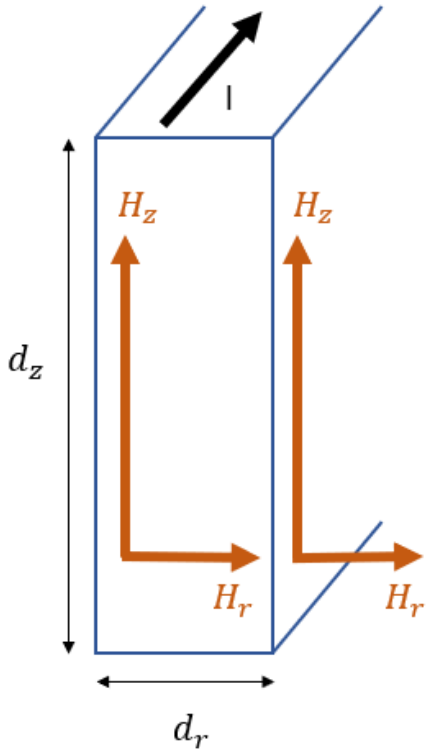

Figure 4.2: Conductor under study to calculate eddy current losses within [6]

The magnetic field intensity values obtained are then further post-processed and are used to calculate the power loss density (power loss per unit volume) due to eddy currents at each section through the following expressions [1] for the axial and radial components respectively:

$$p_{(eddy,z)} = \frac{H_z^2}{d\sigma\delta}\left[\frac{\sinh\frac{d_z}{\delta} - \sin\frac{d_z}{\delta}}{\cosh\frac{d_z}{\delta} - \cos\frac{d_z}{\delta}}\right] \tag{4.2}$$

$$p_{(eddy,r)} = \frac{H_r^2}{d\sigma\delta}\left[\frac{\sinh\frac{d_r}{\delta} - \sin\frac{d_r}{\delta}}{\cosh\frac{d_r}{\delta} - \cos\frac{d_r}{\delta}}\right] \tag{4.3}$$

where is the conductivity and is the skin depth of the conductor,
H_z and H_r are the peak axial and radial field intensity, respectively, at the midpoint of a section and,
d_z and d_r are the radial and axial width of the conductor, respectively.

Please take note of the fact that the number, dimensions and placement of sections considered within a winding set area are much different from that of the actual conductors used for the windings of the transformer.

The total eddy current losses in each winding set are then calculated by multiplying the power loss densities calculated at each point, with the volume of that section when revolved around the axis of symmetry of the equivalent model. The value obtained is further multiplied by a correction factor that takes into account the spatial distribution of strands of conductor within winding area given by:

$$c = NA_t / A_w \tag{4.4}$$

Where N is the no. of turns in the winding,
A_t is the cross-sectional area of a turn of the winding, and,
A_w is the cross-sectional area of the entire winding set.

4.1 LITERATURE REVIEW

Before moving onto the implementation of the above discussed approach to calculating eddy current losses in windings, it would be well-advised to have a look at other approaches to finding the eddy current winding losses found in literature. This subsection will, thus, provide a brief on each such approaches. These have been studied for normal operating conditions for the transformer and when it's not under GIC.

Among the researchers who have delved deep into this case, it has been R.L. Stoll whose contribution has been significant, who has released a book on it. In his paper published in 1967 [18], he expounds on the use of numerical methods, especially, finite difference methods that focus on successive over-relaxation using digital computers. These numerical techniques, he explained, could help validate simplifications in approaches. But, the finite difference method was slow to converge because the relationship between the current density and the magnetic vector potential were a bit complex for that time. He proposed to overcome the convergence issue by forcing the magnetic vector potential in the boundaries.

In 1969, Stoll again released a paper [19], deriving the equation to calculate the eddy current losses in a conductor with rectangular cross-sectional area. This formula, however, failed to hold true for dimensions of the conductor beyond 6 times its skin depth. The derived formula was

based on the assumption that the field is perpendicular to the sides of the conductor and with the used of unknown exponential variables, that eventually is made to depend only on the conductor dimensions and skin depth.

When Stoll published a book dedicated to The Analysis of Eddy Currents [20], which derives the governing equations for both the axial and radial components of winding eddy current losses of rectangular conductors that were stated in the previous section for use in this thesis. These equations were derived on the basis on first principles and the use of one-dimensional solution of the field. The differential field equations obtained were then made to result in a diffusion equation after much simplifications.

Kulkarni et al [21] moved to explore the usage of FEM to calculate winding eddy losses through the determination of leakage field but failed to accurately model their distribution around the boundaries of the winding. In a recent development, Kulkarni et al [22] developed a calculation method for eddy current losses that makes use of electric field, the results obtained from which were close to that obtained by Stoll.

M.C. Haltshwayo in [16], explores the effect of the size of the core window on the winding eddy losses but doesn't exactly quantify their relation through an equation. The effect of the size of the core window on the winding eddy losses will be briefly touched upon in this thesis after verifying the decided-upon method to calculate them.

4.2 EDDY CURRENT LOSS CALCULATION USING ANALYTICAL FORMULA IN PYTHON

The post-processing of the field values obtained from COMSOL was done using Python programming language, the code for which can be found in the Appendix for the GIC case.

Before proceeding with calculating the eddy current losses in the windings due to GIC, the code was first verified for full-load condition of the transformer, the winding losses value for which were available from the company while that for GIC condition wasn't.

To achieve the full-load condition of the transformer in COMSOL, the following connections as shown in Fig. 4.3 were made using the Electric Circuit interface and the ohmic load was adjusted until the full-load current corresponding to each winding flowed through them. A transient simulation using a time dependent study was carried out for the first 3 cycles.

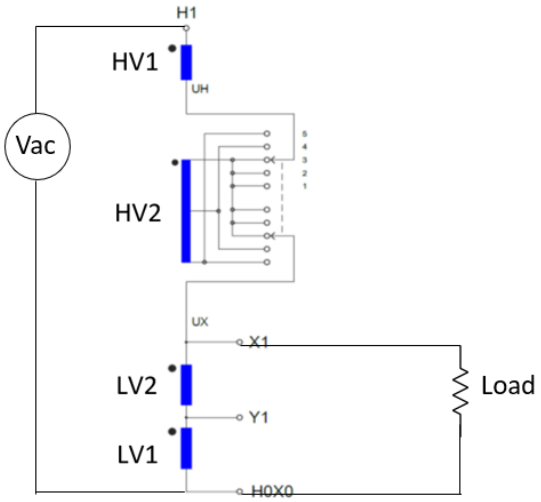

Figure 4.3: Full-load condition connections under consideration

At the desired points across each winding set as mentioned before, the positive peak of the last cycle of the axial and radial magnetic field intensity was obtained and the losses were calculated as follows (tables 4.1 & 4.2) and were checked against the losses obtained by the company:

	LV1	LV2	HV1	HV2
Axial loss (kW)	0.07	7.2	8.4	0.11
Radial loss (kW)	2.3	6.9	2.1	0.32

Table 4.1: Analytical formula eddy loss values for no GIC condition

	LV1	LV2	HV1	HV2
Axial loss (kW)	0.1	7.0	8.1	0.1
Radial loss (kW)	2.1	6.51	1.9	0.3

Table 4.2: Company eddy loss values for no GIC condition

As can be seen, the losses calculated through the simulation is in close agreement with the company values, thus, validating the method used to calculate the losses from the equivalent model.

When moving on to finding the winding eddy current losses under no-load GIC condition (following the same schematic as in Section 3.2.), the increased harmonic content of the leakage field needs to be taken into consideration. Resolving the leakage field into its harmonic components is achieved by plotting the magnetic field intensity at the desired points of each winding over 3 cycles after reaching steady-state. But instead of plotting against time, they are plotted against the frequency spectrum which can be done by simply choosing Frequency Spectrum from the drop-down box in the X-Axis Data section of a Point Graph under 1D plot group. Checking the Scale checkbox under the same section and then plotting gives the RMS value of the field intensity for all the harmonics as shown in Fig. 4.4.

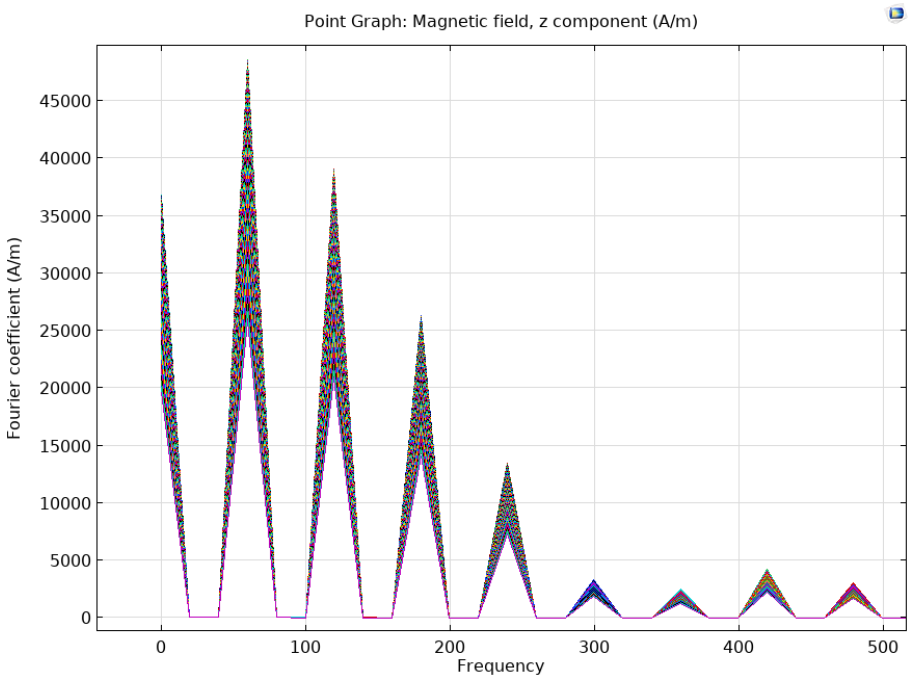

Figure 4.4: Field intensity FFT at all the 2D cutpoints considered

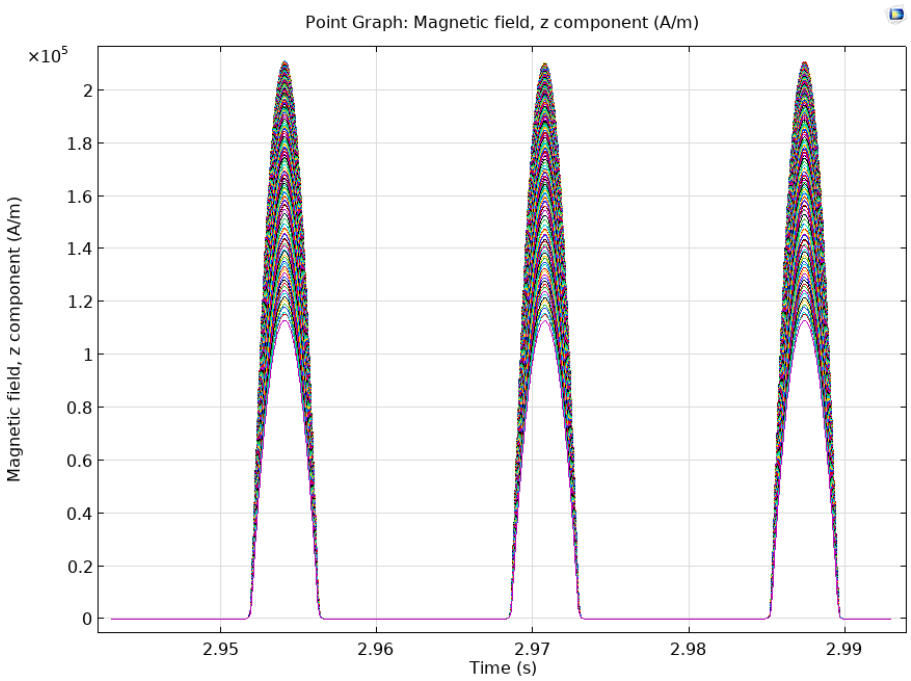

Figure 4.5: Field intensity waveform at all the 2D cutpoints considered

The harmonic components obtained at the desired points is then post-processed to calculate the losses. The Python code implementing the equations 4.2 & 4.3 is modified to find the losses at each frequency component and ensure that at each frequency the skin depth is freshly calculated.

It is to be noted that the magnitude of harmonic components given by COMSOL after following the above steps is actually the RMS value of each component, and thus, need to be multiplied by a factor of $\sqrt{2}$ in the post-processing in Python.

Since there aren't company values for the losses under GIC are available to verify this modified code for GIC against, only the LV winding in the FEM model, which was previously just represented by a rectangle in the equivalent model was now made more detailed.

4.3 DETAILED FEM MODEL TO SIMULATE EDDY CURRENT LOSSES FOR VERIFICATION

In the detailed model, each strand of each turn of the winding was represented by their original dimensions and were spaced equally through winding area, as shown in 4.6. This was achieved in COMSOL by using the Array feature under Geometry.

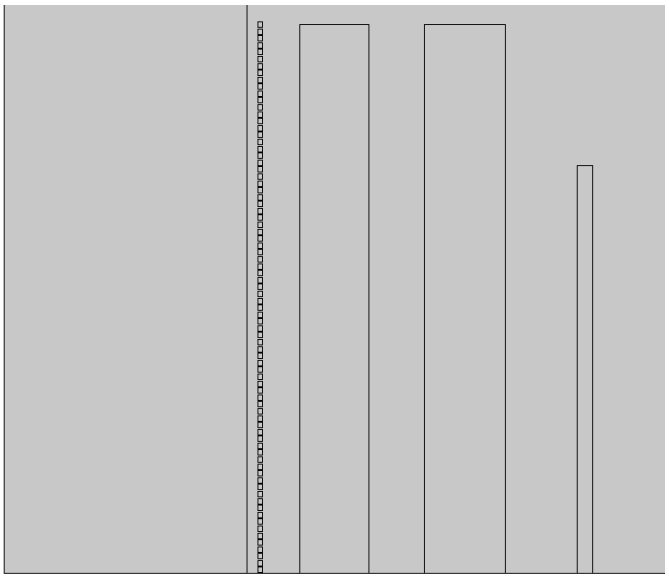

Figure 4.6: Geometry of detailed LV1 winding for eddy current loss calculation

In order to save time while computing this detailed model, the magnetizing current plotted over time for the simulation run with the equivalent model previously was exported for one cycle after reaching steady-state into a text file. The magnetized current values against time was imported to the detailed model as a function of time. To achieve this, under Definitions in the Model Builder window of COMSOL, an Interpolation function was added. In the settings window under the Definition section, Data Source can be chosen as file and the exported file containing the magnetizing current values over time is then selected to import. Refer 4.7 for one such magnetizing current waveform imported using interpolation function.

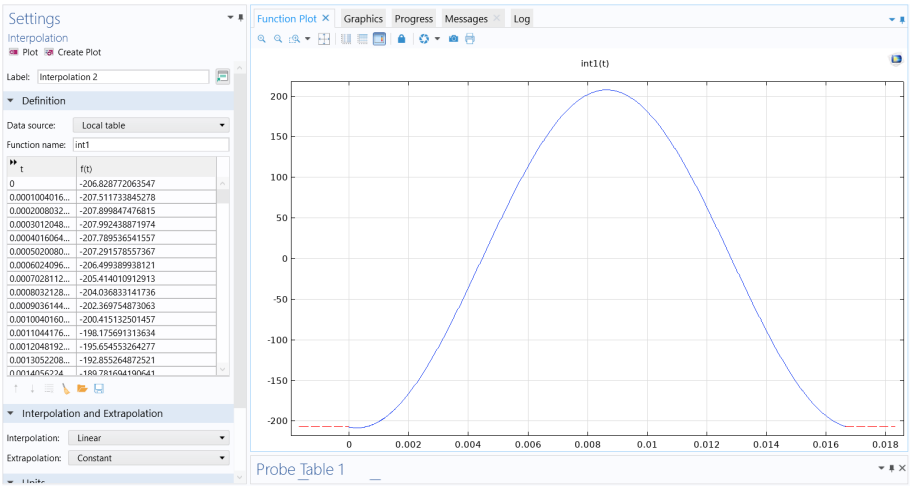

Figure 4.7: Magnetizing waveform imported using interpolation function

The following changes were made to the Physics Interfaces from the previous model:

- While using this method of using magnetizing waveform from previously simulated model, the Electric Circuit interface is no longer needed, as this magnetizing current as a function of time would be fed.
- Under the Magnetic Fields interface, all of the strands' domains together were selected as one coil.
  - Under the settings window of the coil, under Material Type section, their material type is chosen as Solid since it is no more a rectangular space roughly indicating evenly distributed strands but more detailed where each individual strand is modelled.
  - For similar reason, under the Coil section, Conductor model is chosen as Single Conductor.
  - The Coil Group option is then checked to indicate all of the strands are connected in series, since by default it is assumed they are connected in parallel.

    No matter the number of strands within a turn, all of the strands in the winding set need to be connected in series so that the current flow in all of them need to be in the same direction. If every set of strands making up a turn were to be connected in parallel, i.e., uncheck the Coil Group option, the simulation would assume that eddy currents circulate within the set of strands making up the turn and not within each strand as in the real scenario.
  - The Coil excitation is chosen as Current, and in the Icoil field that appears, the function name of the Interpolation function specifying the magnetizing current values is given with its argument as 't', i.e., output times of the simulation solver. This value needs to be divided by the number of strands in a turn for the transformer.
- The settings for the other windings remain as before except their Coil Excitation as well is chosen as Current, and the name of the Interpolation function is specified in the Icoil field as shown in 4.8.

As the purpose of the detailed modelling is to as accurately model the eddy currents as possible, the meshing for the detailed LV1 winding needs to be modified such that the mesh elements near the edges of the strands are smaller than its skin depth at the maximum frequency contributing significantly to the losses. This can be found from the frequency distribution of the magnetic field intensity in the previous GIC model. For the model considered in this thesis, that maximum

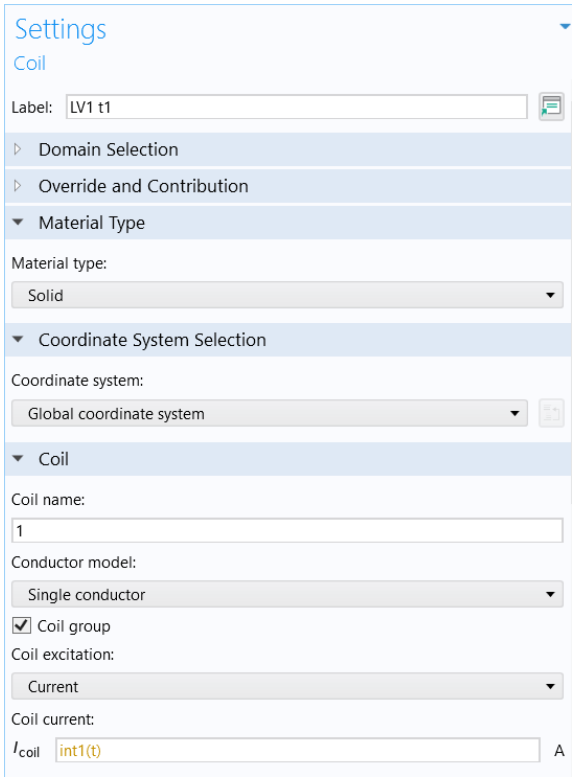

Figure 4.8: Settings for coil

frequency was around 600 Hz. Thus, at least three layers of mesh elements near the boundaries of the strands of the LV1 winding need to have width close to the skin depth at that value of frequency. This was achieved by implementing the following changes to the mesh settings:

- To determine the number of mesh points on the edges of the strand domains, an Edge subnode is added to the Mesh node and the boundaries of the strands are selected. Under Edge, a Size subnode is added, under the settings of which, under Element Size Parameters, Maximum Element Size is checked and in the field that appears the maximum desired size between two mesh points should be specified, which should be lesser than the skin depth at the highest frequency considered.
- A Boundary layers subnode is added to the Mesh node, under which a Size subnode is added. In the settings window for Size, under the Boundary Layers Properties section the number of layers should be given as minimum 3 and the Thickness is specified as the same value mentioned for Maximum Element Size for the Edge subnode.

After the changes in mesh settings, the mesh should look like the Fig. 4.9 for a strand of the conductor turn.

In the Time-Dependent study, the same settings for the solver were kept as in the previous simulation except the starting and ending output times taken by solver were modified to match the starting and ending times of the sampled magnetizing current from the previous simulation run, given as a function in this detailed model.

In order to calculate the losses after running the model, the volumetric loss density in the LV1 winding needs to be integrated over the volume of the revolved geometry of the 2d axisymmetric model. For this, under Definitions node, an Integration subnode is added. In its settings window, the domains of the entirety of the LV1 strands are chosen and the checkbox labelled

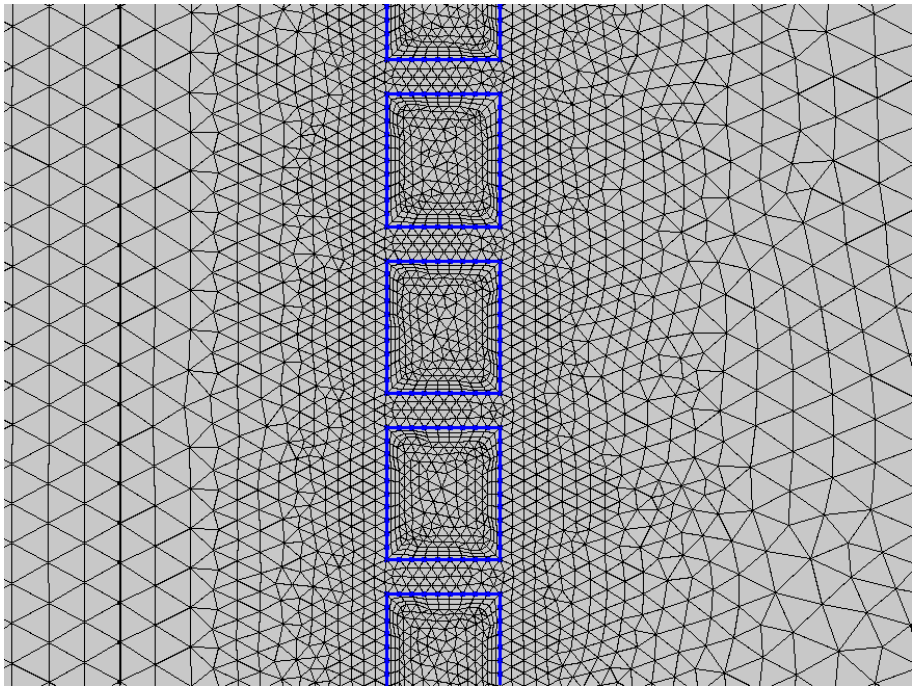

Figure 4.9: Meshing for detailed winding with boundary layers

Compute integral in revolved geometry is checked.

With this level of detail, this model would give accurate eddy current losses as opposed to the equivalent model in COMSOL because it takes into account the interaction of the strands in the winding with one another as well the skin effect through fine meshing near the winding strand boundaries and the effect of leakage field on them.

The difference can be noted when the surface plot of the current density is plotted for the detailed LV1 windings (Fig. 4.10) and that for the equivalent winding (Fig. 4.11). As can be observed, the current density varies within each strand of the detailed model, whereas for the equivalent model, it remains the same throughout for it considers the strands to be roughly uniformly spread over the mentioned area. If the volumetric loss density for the equivalent model is integrated over the volume it only gave the DC resistive losses as the total losses, without the eddy current losses.

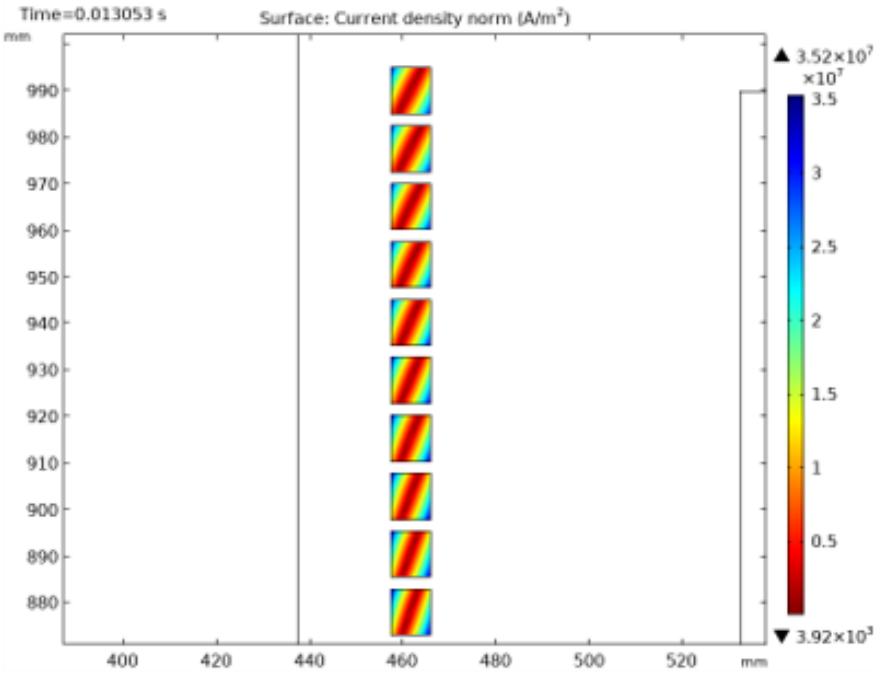

Figure 4.10: Current density in LV1 winding for the detailed model

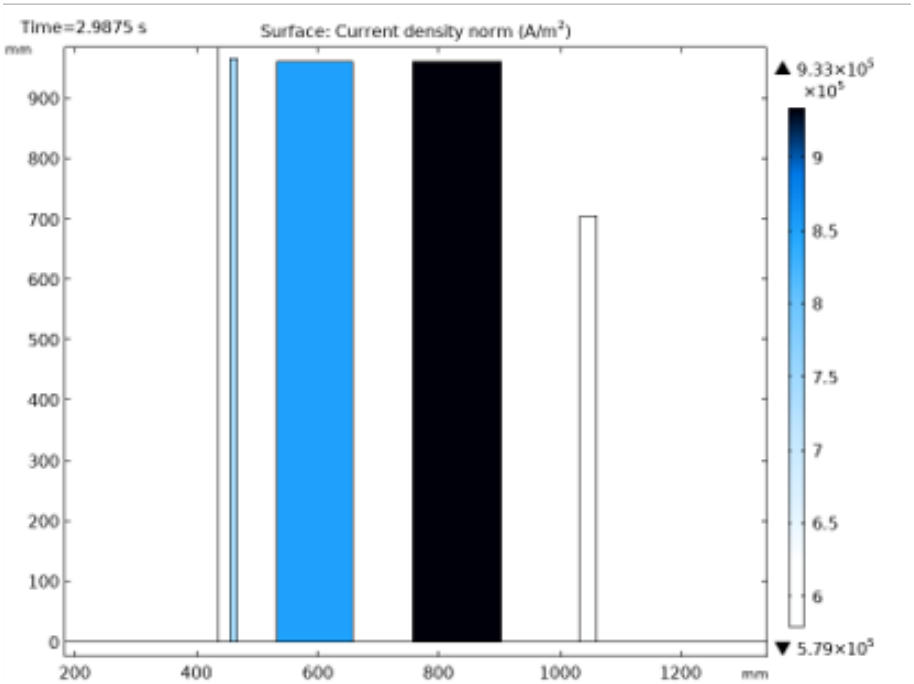

Figure 4.11: Current density for windings in the equivalent model

The expressions for the time-average volumetric eddy current power loss density of the conductor as derived in Section were obtained after relating current density to magnetic field intensity through the following expression which is the time average of the volumetric power loss

density of a conductor over a cycle of the influencing alternating field is given by:

$$P = \frac{1}{2d\sigma} \int_{-\frac{d}{2}}^{\frac{d}{2}} |J|^2 \, dx \tag{4.5}$$

The above expression is the principle behind eddy current loss calculation in COMSOL as well, and with the equivalent model, the imposed current density due to the leakage flux is not considered, prompting the need for a detailed model to verify the analytical formula.

4.3.1 Full-load Condition Without GIC

Before running the detailed model for GIC condition, it is run for the full-load condition to verify if the results obtained from this method is correct. This means the magnetizing current values given to the detailed model will be obtained from the results of the equivalent model with the Electric Circuits interface. It is to be noted that for full-load condition, the magnitude and direction of the magnetizing current in them are different for each winding and care must be taken while mentioning their values before running the simulation.

The model was then run for the full-load condition. To calculate the time-average of the eddy current losses in the LV1 winding, a Global graph under a 1D Plot Group added under the Results node is used to plot the volume integral of the Volumetric electric loss density. This is done by specifying the Expression under the y-Axis Data section as the Operator name of the Integration function defined under Definitions with the argument to the function given as 'mf.Qh' which is the Volumetric electric loss density computed by COMSOL, containing both the radial and axial components of the losses. This expression yields the total losses in the windings, which is equal to the sum of the eddy current loss as well as the DC resistive losses. Thus, the I_2R losses need to be subtracted from the total losses before plotting (Fig. 4.12).

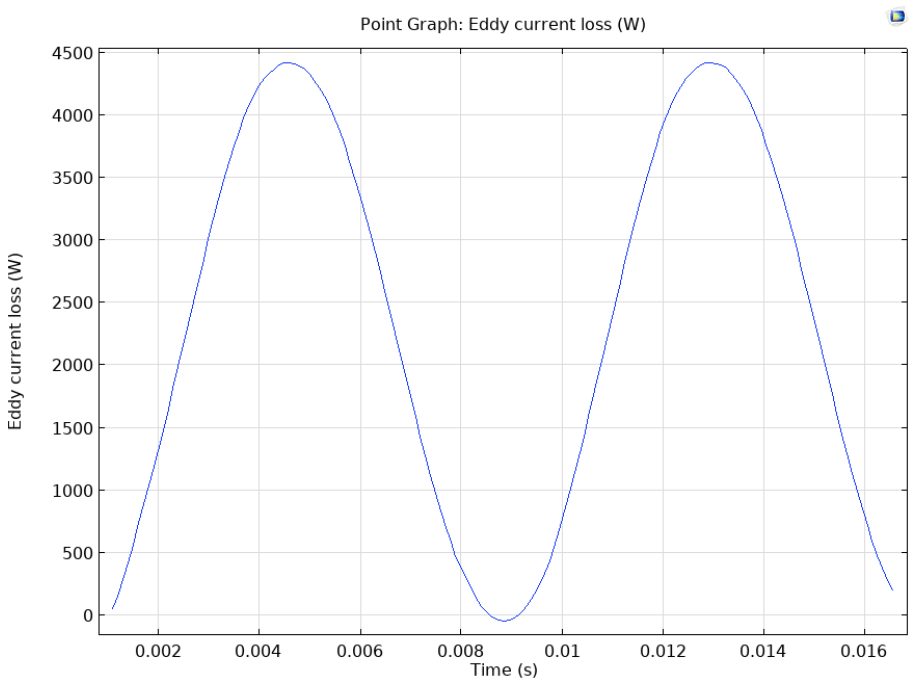

Figure 4.12: Eddy current loss waveform in LV1 winding under full-load without GIC obtained from detailed model (for one cycle of magnetizing waveform)

The plot obtained is then exported to MATLAB and the time average of the eddy current loss

is simply found by finding the mean of the values exported. The mean obtained for the above plot was 2.382 kW. For the full-load condition, this seemed to match the loss value for the LV1 winding found through post-processing in Python and thus, company's loss value for the winding as well (refer tables 4.1 and 4.2). Thus, this validates the method of loss calculation through the analytical formula.

Dependence of winding eddy losses on the core window size

As was mentioned in the literature review of this chapter, [16] has explored the dependence of the size of the core window in real life scenarios on the eddy current losses in the windings. When extended to FEM modelling using equivalent 2D axisymmetric geometry of the core that results in a difference from the real core window size, the losses calculated via the FEM modelling might not emulate the real-life scenario.

The core window size dependence was observed when the company values for the losses did not initially match with the ones found through COMSOL in this thesis. This is because the company does not use an equivalent geometry for the core in their FEM software and thus the core window size remained true to that of the real-life transformer. Once the company changed the core window dimensions to that used in this thesis, the values matched.

To understand this behaviour, comparing the flux lines for both the cases of core window sizes as shown in Fig. 4.13 will help.

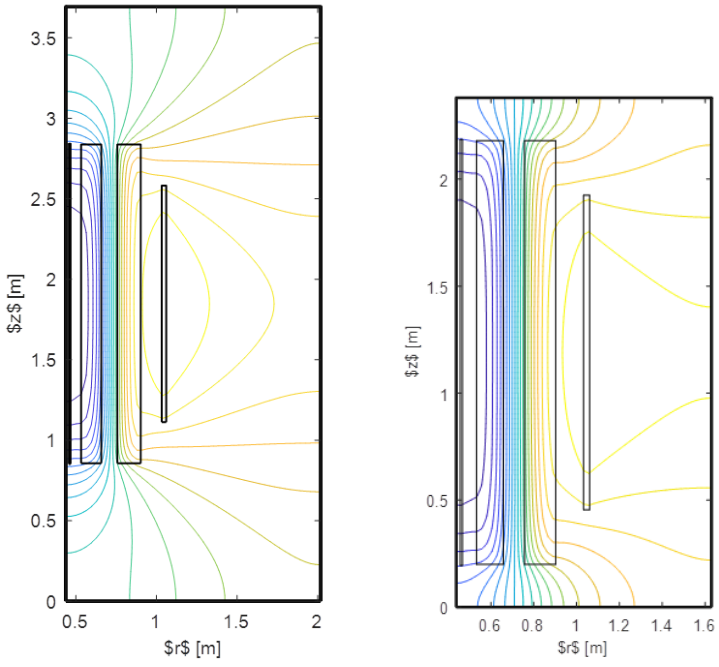

(a) Equivalent core dimensions **(b)** Real core dimensions

Figure 4.13: Influence of core window dimensions on the flow of flux (*Courtesy of Royal Smit Transformers*)

As can be observed from the figures, the flux lines tend to flow easily into the top and bottom core limbs, i.e., more so in the axial direction than in the radial direction. Since for the equivalent core window case, the core window height is higher, the flux lines tend to take the shorter route to the main core limb resulting in comparatively higher radial component than the axial component. Since winding eddy losses depend on the radial and axial components of the leakage flux, the effect of the core window size need to be looked into, especially when trying to model

an equivalent geometry for the core. But this isn't within the scope of this thesis, and is left for future scope of work.
Another aspect to consider is that with 2D axisymmetric geometry it would imply that with its revolution the windings would be encased by the outerlimb and flow of flux would be affected and thus the losses in the windings. Studying these factors would also allow for future scope of study.

4.3.2 No-Load Condition With GIC

The detailed model was then run for the GIC condition by again using the magnetizing current values imported from the equivalent model in GIC condition, for 3 cycles. The time-average of the eddy current losses in the LV1 winding (Fig. 4.3.2) was found just as in the above case, and as can be seen from the below table, the values indeed match with the eddy current losses calculated through the analytical formula implemented through Python which was around 30kW.

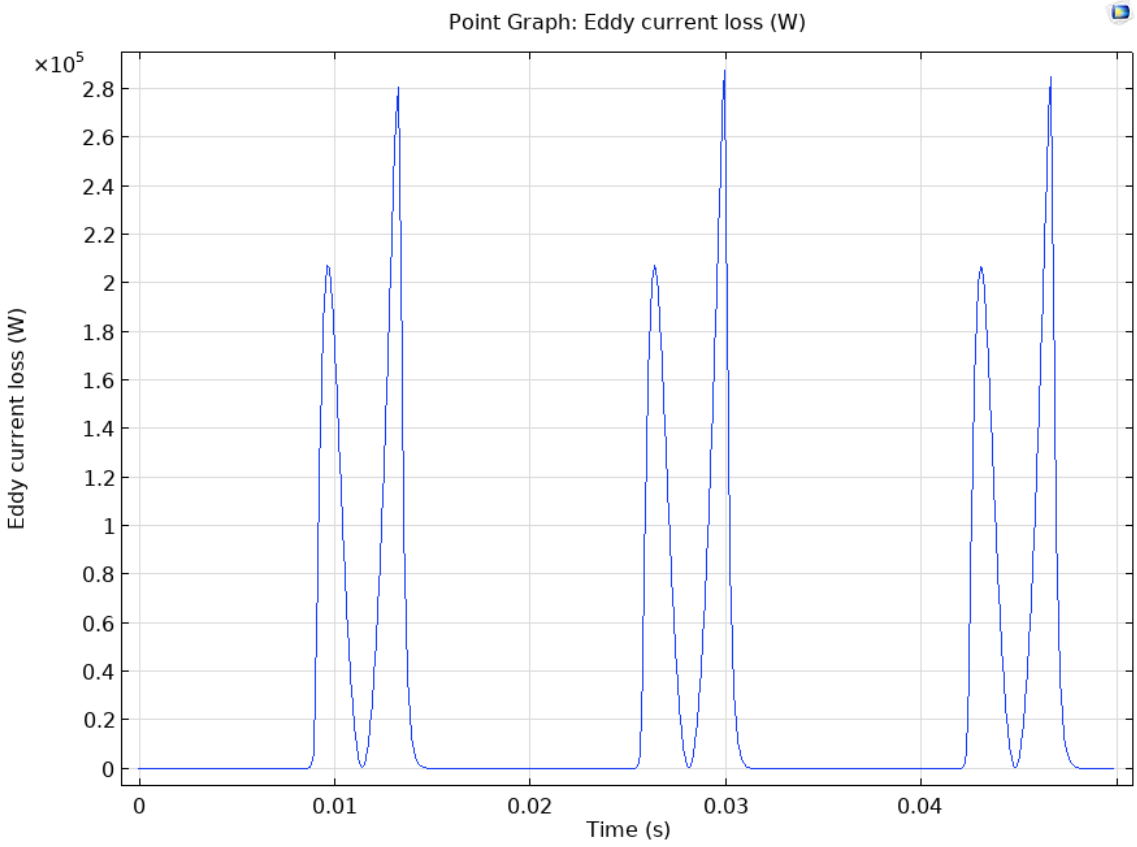

Figure 4.14: Eddy current loss waveform in LV1 winding under no-load with GIC obtained from detailed model (for three cycles of magnetizing waveform

The following table 4.3 shows the losses in the rest of the windings of the windings of the transformer, found through the analytical formula:

	LV1	LV2	HV1	HV2
Axial loss (kW)	30.4	7.9	1.3	0.9
Radial loss (kW)	0.7	9.3	9.9	0.7

Table 4.3: Analytical formula eddy loss values for GIC condition

Comparing the trend of magnitude of axial and radial losses among the windings for the case with GIC in Table 4.3 to that in the case without GIC in Tables 4.1 and 4.2, it can be observed that in the former case the highest axial losses are towards the winding closest to the core, i.e., LV1 winding while the axial losses are the highest in the middle windings (LV2 & HV2 windings) for the latter case. The trend in radial losses however seems to remains the same for both cases, i.e., highest in the middle.

This can again be attributed to the distribution of flux lines in both the cases. As can be observed in Fig. 3.9a for the no-load GIC case, the gray lines representing the flux lines, have the highest axial component near the LV1 winding but they are the highest in the middle for the full-load no-GIC case shown in Fig. 4.13. Thus, the magnitude of losses in the windings would also depend on the connection of the windings.

An interesting observation regarding the shape of the eddy current losses waveform over time in Fig. 4.3.2 is that its shape differs from the full-load condition observed without GIC in Fig. 4.12. While in the case without GIC the losses follow a smooth sinusoidal shape, the losses for the case with GIC peaks before and after the time corresponding to the peak of the positive cycle of its magnetizing wave, because the losses are proportional to current density (refer 4.5) which in turn is proportional to the derivative of field intensity H, as per Maxwell's equation:

$$\nabla \times \vec{H} = \vec{J} \tag{4.6}$$

Since the field intensity follows the shape of the magnetizing waveform, the places where the slope of the waveform is high, the losses will also peak. In the case without GIC, the slope follows the shape of the waveform, but due to the heavy presence of harmonics in the case with GIC, the loss waveform exhibits the peaky behaviour as in Fig. 4.3.2.

5 TIMESAVING APPROACH TO OBSERVE TRANSIENT PHENOMENA OF GIC IN TRANSFORMERS

As is established by now, it takes a few seconds for the transformer to reach steady-state when subjected to a quasi-DC current like GIC. But it is also established that, in order to simulate this from zero time till steady-state time using an 2D axisymmetric FEM model in COMSOL, it is done so at the rate of 1 hour of run time to simulate 1 second of the phenomena. While, thus far, this time consuming way was thought to be the only way to observe the phenomena of GIC in a transformer in this thesis, a timesaving approach was stumbled upon when trying to verify the shape of the magnetizing current waveform of the transformer under GIC in the no-load condition using MATLAB Simulink. With this timesaving method, a lot more about the GIC phenomena in transformers under no-load condition could be observed, as will be entailed in this section after elucidating the steps followed to achieve this.

5.1 OBTAINING THE FLUX VERSUS CURRENT CHARACTERISTICS OF THE TRANSFORMER CORE FROM FEM MODEL

Under no-load condition, the transformer behaves as an inductor connected to a voltage source. Since the saturation characteristics of the transformer becomes imperative to observe GIC, a non-linear inductor will be used in the circuit implemented in MATLAB Simulink to represent the non-linear magnetizing characteristics of the transformer core, following the principles of a magnetic equivalent modelling discussed in Chapter 1. The type of magnetizing characteristic taken by this non-linear inductor in Simulink is by way of Flux versus Current characteristics rather than the Magnetic Flux Density versus Magnetic Field Intensity characteristics. Using Flux vs. Current characteristics also ensures that it takes into account the geometry of the transformer core while the Flux Density (B) vs. Field Intensity (H) characteristics are dependent on the core dimensions.

But, only the B vs. H characteristics of the core material are available with the company. Thus, the MATLAB Simulink model cannot be implemented directly. FEM modelling would still have to be done but not to the extent as described before. The Phi vs. I characteristics of the core would have to be obtained by imparting the available B vs. H characteristics to the equivalent 2D axisymmetric model of the transformer.

This is done by modelling the geometry and material properties as mentioned in Section. The Magnetic Fields Physics interface settings also remain the same, except the Coil Current excitation is changed to simply 'Current'.

The goal is to see the amount of flux in the core for varying magnetizing currents. This means that the current supplied to the windings need to be swept through the desired range of values. This can be achieved adding a Parametric Sweep study step to a Stationary Study. A new variable must be added under Definitions node by choosing the Variables subnode, and mentioning the variable name of the variable to be swept over and its units in the settings window. Since we are interested in sweeping over the magnetizing current, the variable created for this would be entered in the Icoil field under Coil Excitation in the settings window of the Coil domain

condition defining the windings in the magnetic fields interface.

For this auto-transformer under study in this thesis, since no-load condition implies all of the windings connected in series with the voltage source, the same current is given to all of them.

In the Parametric Sweep study step under Stationary Study, the variable to be swept over is added and the range of values to be swept over is also specified as shown in Fig. 5.1. While deciding this range of values, care must be taken to ensure that the step mentioned for the range of values during and before knee point of the curve be as small as possible without resulting in a lot of steps, which can be achieved through a few trials and errors. This is done because, before knee-point the curve might appear linear, it is actually ever so slightly curved and flux in the core changes drastically for a slight change in magnetizing current at this stage. But after reaching saturation after the knee point, the curve is pretty much linear and the step size at this stage can be chosen to be fairly large for the input magnetizing currents.

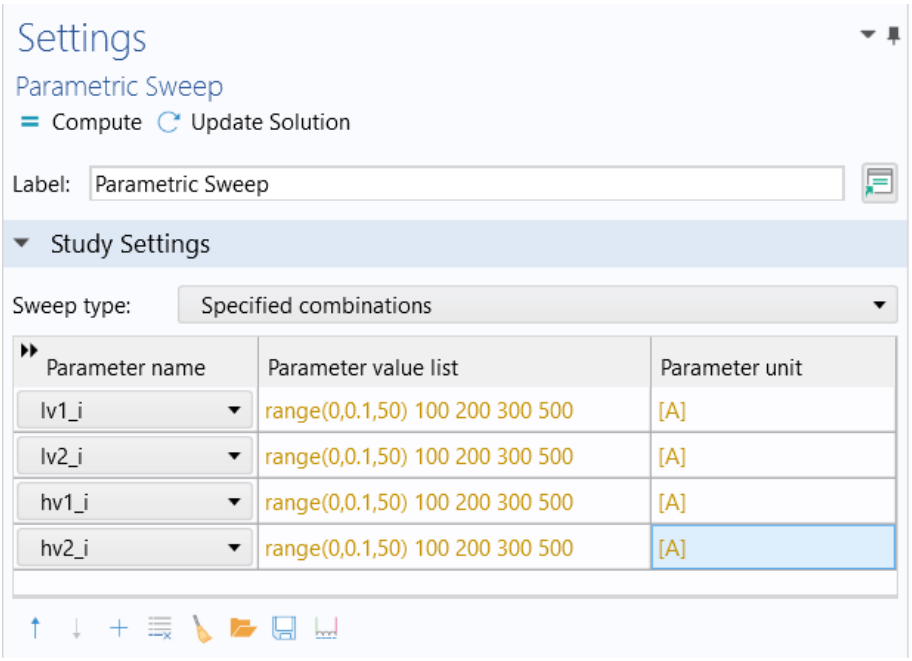

Figure 5.1: Range of magnetizing currents specified to measure the flux vs. current characteristics

Once the parameter values have been specified, the model can be computed. This takes around half an hour or so, for the auto-transformer model considered in this thesis. Once it's done computing, in the Results node, using a Global graph under a 1D Plot Group, the flux vs. current characteristics are plotted as shown in Fig. 5.2. To do so, the Expression in y-Axis Data is set to the sum of the flux in all the windings (usually denoted by mf.PhiCoil_x where x is the Coil number of the winding) and the Expression in x-Axis Data is set to the current through any one of the winding sets (mf.ICoil_x). This plot is the exported as a text file to be used in MATLAB Simulink. Since only half of the geometry of the transformer is simulated, the flux values will have to be multiplied by a factor of 2 when using in Simulink.

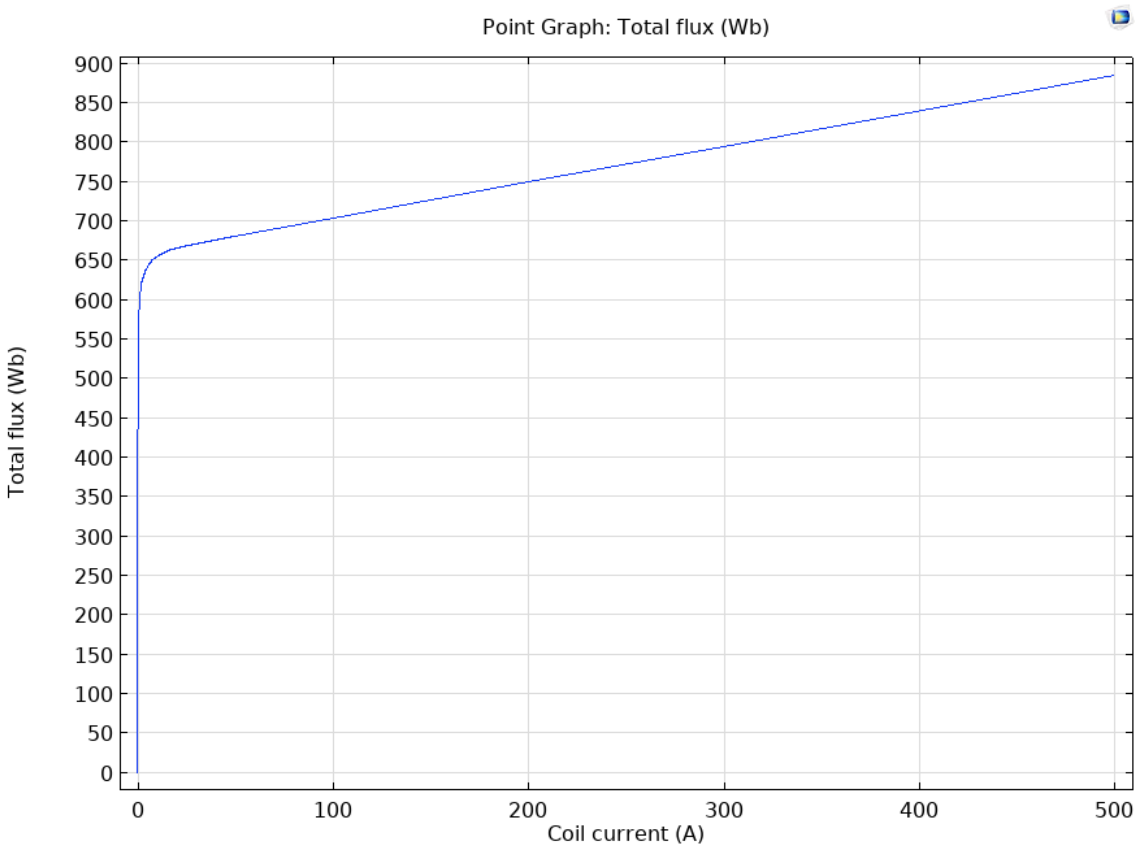

Figure 5.2: Flux vs. Current characteristics obtained

5.2 RUNNING THE TRANSIENT SIMULATION IN SIMULINK AND OBTAINING THE MAGNETIZATION CURRENT UNDER NO-LOAD CONDITION

As mentioned before, the no-load condition of transformer under GIC would be represented by a non-linear inductor with a voltage source in series. The circuit should look like the one shown in Fig. 5.3. The details of each component in the circuit representing the condition is listed below:

- For the AC voltage supply, a Controlled Voltage Source. It is controlled by a Sine Wave block whose amplitude was set to $525\sqrt{\frac{2}{3}}$ kV, frequency to $2\pi 60$ rad/sec and phase to $\frac{\pi}{2}$ to avoid build-up of inrush currents.
- For emulating the GIC, again, as in the case of COMSOL model, a DC voltage source in series with a resistance is given. To manipulate the value of GIC, only the amplitude of the DC voltage source is changed while the resistance is kept constant.

  For the DC voltage source, again, a Controlled Voltage source is used – mainly to supply the DC source after the system has settled from starting with the AC source and to supply the DC source with a ramp with slight slope so that its effects become noticeable.

  The Controlled Voltage Source is controlled by a Switch block which has three inputs. To the first input, a Constant block with its value set to the GIC voltage is given. To the second input, a Clock block is given which gives the current simulation time. To the third

input, a Ramp block is given, who start time and slope is specified such that the ramp starts only a few milliseconds before the Constant block is passed through, and the slope given must be the Constant block's value divided by the interval between the start of the ramp and the passage of Constant block. The criteria of control for the Switch is such that the first input is passed through if the second input satisfies the criterion specified in the Switch block. Here it will be done if the output of the Clock is greater than 1. If the criterion isn't satisfied, by default the third block's output will be passed through.

- A resistive branch is added in series to these whose value should be the sum of the winding resistance as well as the GIC resistance.
- Finally, a Non-Linear Inductor block is added to represent the transformer under no-load condition. To this block, the imported flux versus current characteristics is fed.
- Additionally, a ground node is added and a current measurement block to observe the magnetizing current waveform. A powergui block is added as is needed with all Simulink simulations, and its simulation type must be set to Discrete since the flux vs. current characteristics supplied are discrete.

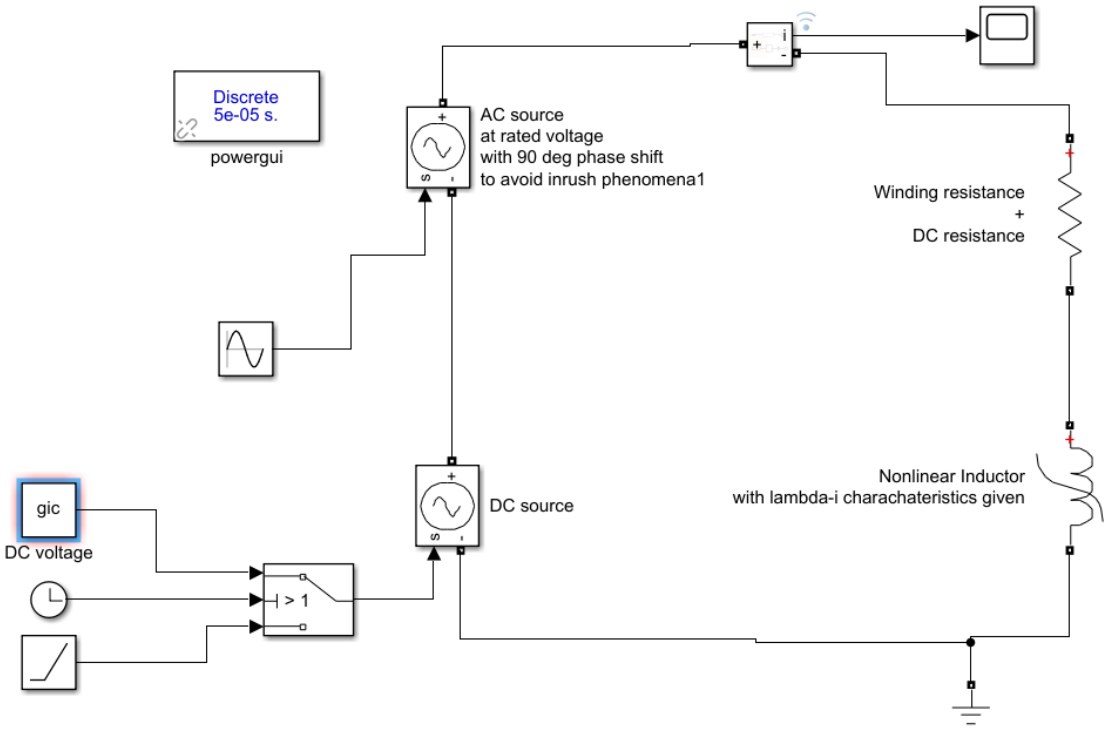

Figure 5.3: Magnetic equivalent circuit implemented in Simulink

5.2.1 Verifying the Simulink model against COMSOL model

To verify if the output magnetizing current waveform magnitude and shape obtained from Simulink is similar to the one obtained with previous COMSOL model, they were compared for three magnitudes of GICs as shown below in the table of figures shown in Table 5.1.

As can be seen, for 25A and 75A GIC, the waveforms in Simulink and COMSOL seem to be in very close agreement but for 50A GIC the magnitude of magnetizing current in COMSOL is lower than that in Simulink. But it can also be observed waveform obtained in COMSOL,

GIC	COMSOL	Simulink
25A	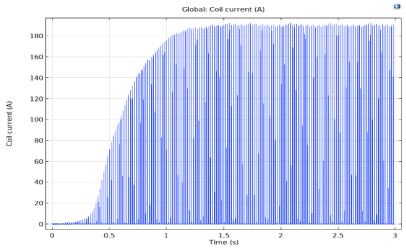	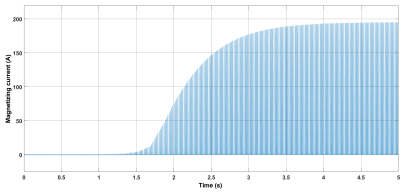
50A	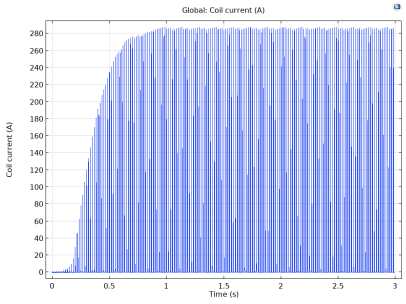	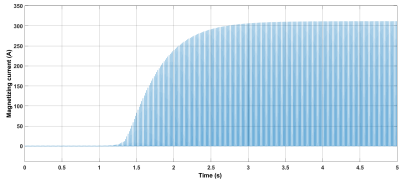
75A	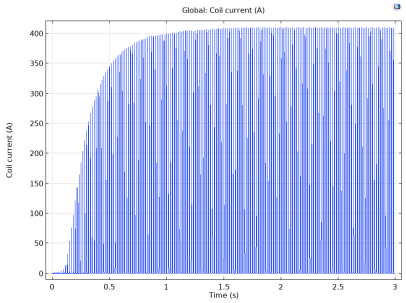	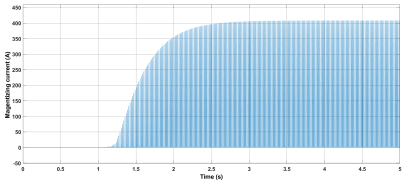

Table 5.1: Verifying Simulink magnetizing current waveforms against those from COMSOL

even after reaching steady-state seems to struggle to have smoother envelope at the top of the waveform, indicating the solver might be struggling to smoothly trace the magnetization curve which may have caused the rather significant difference in magnitude of the magnetizing current between COMSOL and Simulink.

5.3 LOGGING AND EXPORTING THE MAGNETIZING CURRENT FROM SIMULINK

After running the simulation, the values output by the Current Measurement block needs to be stored somewhere. For this purpose, changes in the Modelling tab in the Menu bar of the Simulink Model window are made before running the simulation. In the tab, Model Data Editor is clicked. From the window that shows up, Signals tab is clicked and 'Instrumentation is chosen from the drop-down. A list of the signal blocks should appear, and in that, the checkbox under Log Data column next to Current Measurement should be checked as shown in Fig. 5.4. This will ensure the values that the block outputs is logged and available in the workspace.
After running the model, the following line of code if run in the workspace or using a script in the editor:
`simOutputs(1).logsout1.Values.Time` and
`simOutputs(1).logsout1.Values.Data`,
will give the time outputs and the magnetizing current at those times, respectively. This informa-

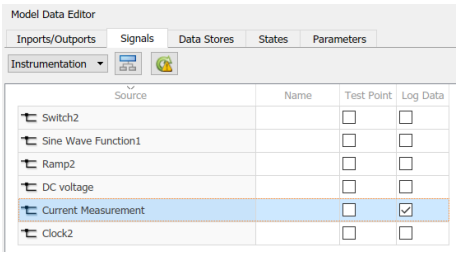

Figure 5.4: Settings to log the magnetizing current obtained in Simulink

tion can then be stored in a text file to be used again in COMSOL to study the electromagnetic behaviour of the transformer core and windings under GIC.

5.4 STUDYING THE ELECTROMAGNETIC BEHAVIOUR OF THE TRANSFORMER IN COMSOL

As was done to simulate the detailed model in COMSOL in Section 4, an Interpolation function is used to specify the magnetization current vs time for the equivalent model described in Section 5.1. The Electric Circuit Physics is no longer needed, as simulating the circuit in Simulink took care of that part. The Interpolation function can then be given as the current mentioned against the Icoil field under Current Excitation settings for the windings in the Magnetic Fields Physics.

Now, the model can be run using a Time Dependent with the same Solver settings as used throughout this thesis for only a few cycles of the imported magnetization current after it has reached steady-state. Either the range of times and their respective currents in the Interpolation function be changed accordingly or the range of times specified for Output steps taken by the Solver in the Time Dependent Study be changed to simulate just those few cycles. For optimum results while studying the harmonics in the transformer, it is ideal to run the simulation for around 3 cycles. After computing the model, the results can processed just as before, and the losses in the windings can be calculated.

For the equivalent model of the auto-transformer model used in this thesis, this resulted in the run time for this section being around 30 minutes. Between extracting the flux vs current characteristics from COMSOL, running the transient simulation in Simulink, extracting the magnetizing current from there, and back to studying the electromagnetic behaviour in COMSOL again the process shouldn't take more than 2 hours to set up the base for further study with the same model of a transformer.

Besides reducing the run-time in general, this method has an edge over using the Electric Circuit Physics and running a transient simulation from beginning to steady-state, because for lower GIC currents the time to reach steady-state is more than a few seconds - as will be discussed in detail in the next section – and since the rate of simulating with that way was found to be around an hour of simulation time for 1 second of real time, it would take several hours before being able to study the behaviour for lower GICs.

With this timesaving method, once the Simulink model is ready for a particular transformer model, the magnitude of GIC it is subjected to can be varied and the magnetization current obtained for various GIC magnitudes can be exported to COMSOL again to study its electromagnetic behaviour at each GIC.

5.5 TIME CONSTANT OF THE TRANSFORMER FOR VARIOUS GIC MAGNITUDES

With the help of this timesaving method, an interesting observation could be made about the time constant of the transformer for increasing magnitudes of GIC. The time constant of this system that resembles an L-R circuit should be L/R, and the time taken to reach the steady-state should be around 5 times of that. The 'L' here being the inductance of the transformer and 'R' being the resistance of the system equal to the sum of the winding resistance as well the resistance added to supply a GIC.

To observe the dependency of the magnitude of GIC magnitude on the system, while keeping the resistance of the system constant, the amplitude of the DC voltage source needs to be varied. This calls for a parametric sweep over the amplitude of the DC voltage source supplied in the Simulink. The following steps are followed to achieve the same:

- In the Simulink model window, under the Modelling tab, Model Data Editor is clicked.
- In the window that appears, Parameters tab is clicked. Next to the Constant block specifying the GIC amplitude, in the Value column specify the variable name for it to be swept over.
- It is ensured that the Log Data is enabled for the Current Measurement block as specified before.

The following Script in the Editor window is executed:

```
gic_vals = [0:1:50 100:100:1000]*10; %range of gic amplitudes to be swept
over

for i = 1:length(gic_vals)
  SimIn(i) = Simulink.SimulationInput('simulink_model');
  simIn(i) = setVariable(simIn(i),'gic',gic_vals(i)); %'gic' is the vari-
able name given in the Constant block
end

simOutputs = sim(simIn);

for i = 1:length(gic_vals)
  plot(simOutputs(1,i).logsout1.Values);
end
```

Running this script displays the plots for each GIC amplitude considered. Here, for few of the GIC amplitudes, the magnetizing current waveforms have been shown in the table of figures 5.2.

As can be observed, with increasing GIC, the time taken to reach steady-state for the system decreases. This can be attributed to the fact that inductance of the transformer is non-linear. For the same AC voltage source supplied, the AC flux curve would remain the same but with increasing GIC, the DC flux would increase and offset the AC flux curve. When this trend is projected onto the flux versus current characteristic of the transformer, the resulting magnetizing currents should reach steady-state sooner for higher GIC since after saturation, even a small change in flux results in a large change in the magnetizing current.

It can also be justified in terms of finding the inductance of the transformer as the slope of

GIC	Magnetizing current waveforms
5A	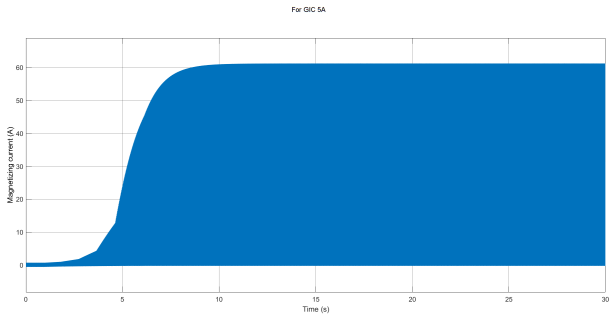
10A	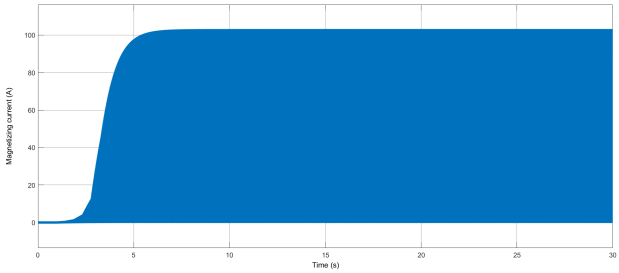
20A	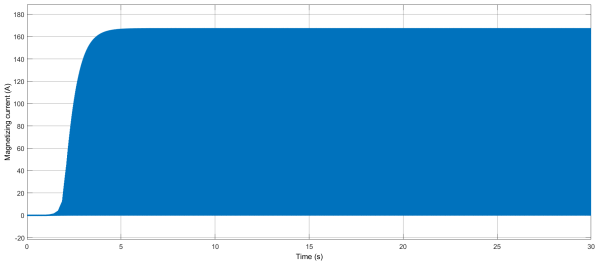

Table 5.2: Magnetizing current waveforms for increasing GIC values

the flux vs. current characteristics, at the level of DC flux produced by a certain amplitude of GIC it is subjected to. The slope remains quite high in the linear region of the graph, implying a high inductance for the transformer operating in that region. But once saturation is reached, the slope drastically reduces resulting in lower inductance for the transformer.

The time constant is directly proportional to the inductance of the system for a constant system resistance and thus, it can be said with increasing GIC, the time taken to reach steady-state decreases.

5.6 SCOPE FOR IMPROVEMENT

The above described timesaving method is far from being perfect and applicable to all cases. Such fallbacks and suggestions for areas of improvement have been elucidated below:

- The timesaving method works just fine as long as the electromagnetic studies that need to be carried out on the transformer are concerned with its operation in the saturation region. But it is not as reliable in the linear operation region. This was found to, mainly, be due to the resolution of the range of currents considered in the linear region (for $\leq$50A) while trying to extract the transformer's flux vs. current characteristics. As can be seen from the flux density waveform within the core found through this method, it is clear that in Simulink the model has had a hard time smoothly tracking the not-so-refined flux vs. characteristics in the region of lower currents fed to it, thus, resulting in the obviously erroneous shape of the flux density waveform as shown in Fig. 5.5.

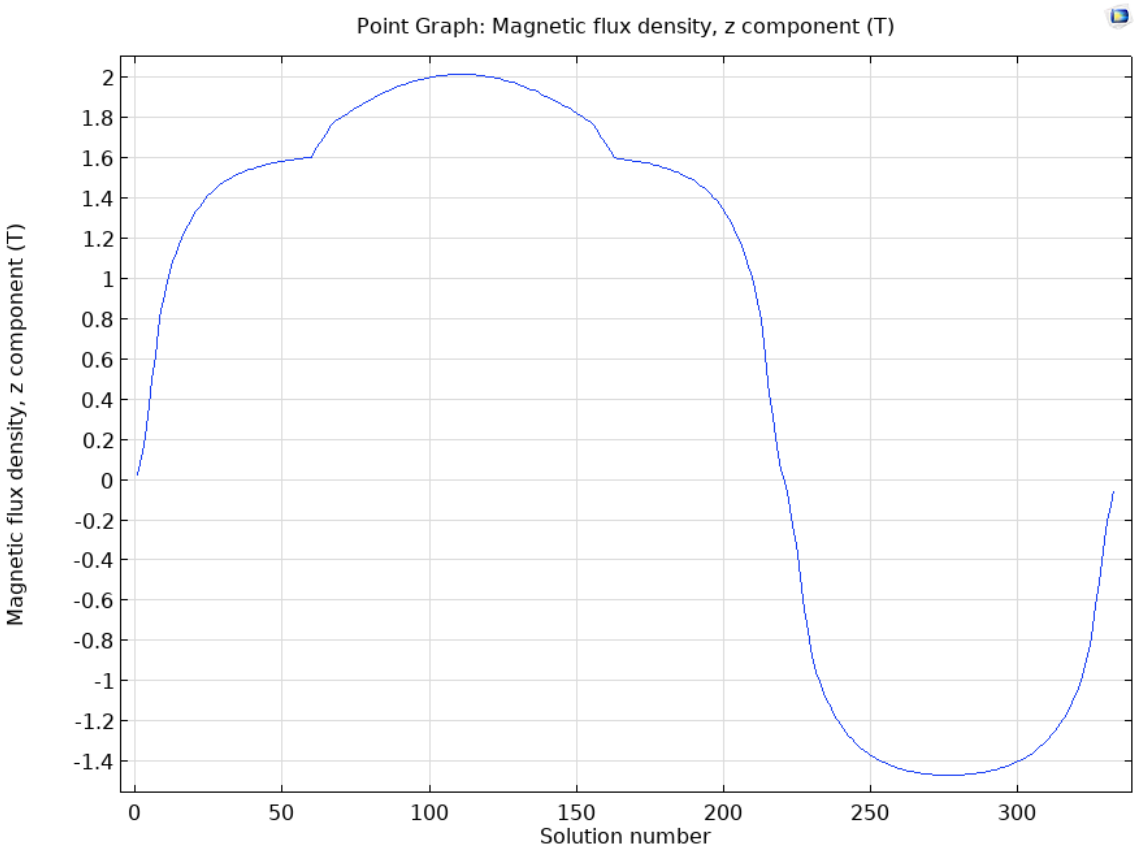

Figure 5.5: Anomalous flux density waveform in the non-saturated regions

This can also be observed if the magnetizing current waveforms obtained through Simulink and through the longer COMSOL method using Electric Circuit interface, particularly in the region where the currents are low, i.e. the half-cycle where saturation isn't observed. We notice that they don't necessarily align with one another and that there is a slight discrepancy present, as shown in Fig.

When the resolution of the range of the lower currents considered was fine-tuned and the flux vs current characteristics obtained from COMSOL was fed to Simulink, inrush behaviour was observed, no matter the mitigation methods employed to diminish them, as can be seen in Fig. 5.6. Thus, a way around this problem needs to be found, as well.

But if the electromagnetic studies need only concern finding the losses in the windings,

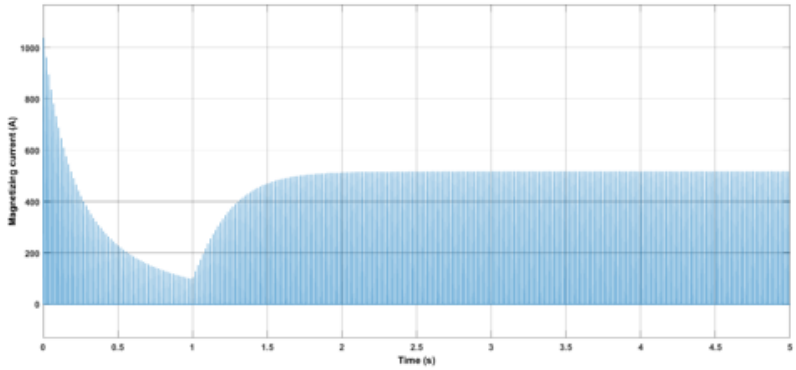

Figure 5.6: Inrush phenomena observed

that include eddy current and resistive losses, then this timesaving method is very much reliable. This is because the magnetizing waveforms obtained for the most part follow closely the waveform obtained through the longer method, and only their shape is mainly of concern to calculate the losses as the magnetic field intensity in the core window, and thus windings, are in phase with the magnetizing current and resemble their shape as well as shown in Fig. 5.7.

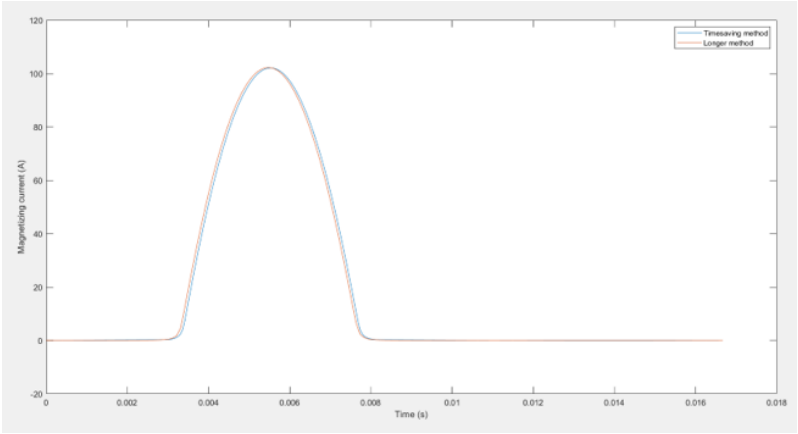

Figure 5.7: Overall agreement of magnetizing current waveforms obtained through straightforward FEM method and through the timesaving method

- This timesaving method, as mentioned before, has only been carried out for the no-load condition of the GIC case with the use of a non-linear inductor in the Simulink model. This would, obviously, not be an accurate representation anymore for loaded condition, where both the primary and secondary coils come into the picture. In that case, the method of measurement of flux vs. current characteristics from the COMSOL model will have to be looked into, and the block to represent this case of the transformer in Simulink will have to be looked into, too. There is a Saturable Transformer block present in Simulink but it asks for the inductance of the windings, which can be tricky to find and mention as a whole, as discussed before, owing to the non-linear nature of it during a simulation itself.

6 CONCLUSION

This thesis has successfully explored how to model power transformers using FEM to study their electromagnetic behaviour, validated the model, and proposed a new modelling method that combines FEM with MEM that has reduced computation time than usual while delivering a model as close to accuracy as possible.

The FEM modelling of the power transformer was done using COMSOL. The model is built such that it emulates the electromagnetic behaviour as close to reality as possible while trying to minimise the computation load with the use of a 2D axisymmetric model. The FEM model faced some shortcomings by way of convergence issues mainly, which were solved by tweaking the solver's settings. The FEM model was then validated for various test cases run on it; especially its electromagnetic behaviour such as its saturation effects was observed for no-load case with and without GIC. Once the FEM model was validated, the spatial distribution of the field intensity in the windings during DC saturation was obtained to calculate the eddy current losses in them, and their results were also validated against a detailed model of the windings that when run in FEM took into account the induction of eddy currents.

Later on in the thesis, the possibility of further minimizing the computation load of the numerical modelling was explored by ensuring the simulation of the transient section of the transformer under GIC phenomena was taken care of by a magnetic equivalent circuit designed in MATLAB Simulink. This modelling method was again validated against the results obtained previously using the first FEM modelling method.

6.1 FUTURE SCOPE OF WORK

While the numerical modelling discussed in this thesis explores the proposal of a timesaving modelling method, it isn't yet robust enough to carry out all kinds of electromagnetic studies and is only a stepping stone to achieve a complete enough model by:

- Extending the FEM model to employ 3D geometry of the transformer and its components, and modify the time-saving method to withstands the shift towards 3D.
- Exploring ways to calculate the stray losses in metallic components of the transformer other than windings such as clamps, magnetic shunt, tank walls, etc.
- Using the timesaving method to arrive at an analytical relation between the time taken to reach the steady-state for a given magnitude of GIC, and the time-varying inductance of the system under GIC when the system resistance is kept constant.
- Studying the effect of size of core window on the eddy current losses in the winding to enable optimal construction of a 2D equivalent geometry of the transformer.

BIBLIOGRAPHY

[1] S. V. Kulkarni and S. V. Khaparde, *Transformer Engineering: Design, Technology, and Diagnostics*. CRC Press, Taylor Francis Group, 2013.

[2] Wikipedia, "Geomagnetic storm." https://en.wikipedia.org/wiki/Geomagnetic_storm#/media/File:Magnetosphere_rendition.jpg [Accessed: 24.09.2021].

[3] L. Borrill, *Duality derived topological model of single phase four limb transformers for GIC and dc bias studies*. PhD thesis, 12 2020.

[4] R. Walling and A. Khan, "Characteristics of transformer exciting-current during geomagnetic disturbances," *IEEE Transactions on Power Delivery*, vol. 6, no. 4, pp. 1707–1714, 1991.

[5] B. Roen, 2016.

[6] S. Mousavi, "Electromagnetic modelling of power transformers for study and mitigation of effects of gics," 2015.

[7] S. Magdaleno-Adame, S. Mokkapaty, and T. D. Kefalas, "Magnetic flux and core loss finite element analysis of electrical steels combinations in lamination core steps of single-phase distribution transformers," 2017.

[8] J. Fink, "Geomagnetic induced current in power transformers: A simplified model for the study of geomagnetic current spectra," in *2017 IEEE International Conference on Computational Electromagnetics (ICCEM)*, pp. 166–168, 2017.

[9] P. Price, "Geomagnetically induced current effects on transformers," *IEEE Transactions on Power Delivery*, vol. 17, no. 4, pp. 1002–1008, 2002.

[10] B. Riemer and K. Hameyer, "Multi-harmonic approach to determine load dependent local flux variations in power transformer cores," *Archives of Electrical Engineering*, vol. vol. 64, no. No 1 March, pp. 129–138, 2015.

[11] N. Chiesa. PhD thesis, Norwegian University of Science and Technology, 2010.

[12] J. Perho. PhD thesis, Helsinki University of Technology, 2002.

[13] M. Amrhein and P. T. Krein, "Magnetic equivalent circuit simulations of electrical machines for design purposes," in *2007 IEEE Electric Ship Technologies Symposium*, pp. 254–260, 2007.

[14] E. C. Cherry, "The duality between interlinked electric and magnetic circuits and the formation of transformer equivalent circuits," 1949.

[15] G. Slemon, "Equivalent circuits for transformers and machines including non-linear effects," 1953.

[16] M. Hlatshwayo, "The computation of winding eddy losses in power transformers using analytical and numerical methods," 2013.

[17] S. M. B. Fossen, "Parallel computing and optimization with comsol multiphysics," 2017.

[18] R. L. Stoll, "Numerical method of calculating eddy currents in nonmagnetic conductors," vol. 114, p. 775=780, June 1967.

[19] R. L. Stoll, "Approximate formula for the eddy-current loss induced in a long conductor of rectangular cross- section by a transverse magnetic field," vol. 116, pp. 1003–1008, June.

[20] R. Stoll, *The analysis of Eddy Currents*. Oxford University Press.

[21] S. K. S.V. Kulkarni, *Transformer engineering: Design and Practice*. 2007.

[22] S. Kulkarni and S. Khaparde, "Stray loss evaluation in power transformers-a review," in *2000 IEEE Power Engineering Society Winter Meeting. Conference Proceedings (Cat. No.00CH37077)*, vol. 3, pp. 2269–2274 vol.3, 2000.

A GIC WINDING EDDY LOSSES CALCULATION USING PYTHON

In [1]:
```
import numpy as np
import math as math
import matplotlib.pyplot as plt
```

In [2]:
```
out_d = np.array([935, 1316, 1807, 2123])
in_d = np.array([912, 1065, 1516, 2067])
rad_th = np.array((out_d-in_d)/2) #radial thickness
ax_ht = np.array([1990, 1980, 1980, 1474])
base_gap = np.array([166,171,171,426])

Nt = np.array([40, 503, 638, 56]) #no. of turns
At = np.array([333.168, 232.87, 181.885, 190.284]) #effective cross-section area of a turn

winding_names = ['LV1','LV2','HV1','HV2']

#half geom
out_r = out_d/2
in_r = in_d/2
core_leg_ht_half = 2380/2

ax_ht_half = ax_ht-ax_ht/2 %(core_leg_ht_half-base_gap)
Aw = rad_th*ax_ht_half #cross-sectional area of winding
Nt_half = Nt/2
c = Nt_half*At/Aw #correction factor

winding_mass = np.zeros(4)

n_rad = np.array([3, 25, 30, 6])
n_ax = np.array([105,100,100,75])

t = (rad_th/(n_rad-1))*10**-3 #SI radial thickness
w = (ax_ht_half/(n_ax-1))*10**-3 #SI axial width
str_ax = np.array([9.9, 7.2, 5.85, 12])*10**-3 #strand axial height
str_rad = np.array([8.5, 1.5, 1.45, 8])*10**-3 #strand radial width
sig = 1/(2.1328*10**-8) #SI
mu0 = 4*math.pi*10**-7 #SI
mur = 1 #SI
no_f = 251 #measured till 5000Hz, at every 20Hz
no_w = 4 #no. of windings
```

In [4]:
```
P_ax = np.zeros((no_f,no_w))
P_rad = np.zeros((no_f,no_w))

for i in range(no_w):
    rad_coord = np.linspace(in_r[i]+rad_th[i]/(2*(n_rad[i]-1)),out_r[i]-rad_th[i]/(2*(n_rad[i]-1)),n_rad[i]-1)
    ax_coord = np.linspace(ax_ht_half[i]/(2*(n_ax[i]-1)),ax_ht_half[i]-ax_ht_half[i]/(2*(n_ax[i]-1)),n_ax[i]-1)
    radv, axv = np.meshgrid(rad_coord,ax_coord)

    coords = np.stack((radv.flat,axv.flat),axis=1)

    Hz_file = np.loadtxt('F:\\Thesis\\Smit data\\Python\\GIC 75A\\FFT\\'+winding_names[i]+'Hz.txt')
    Hr_file = np.loadtxt('F:\\Thesis\\Smit data\\Python\\GIC 75A\\FFT\\'+winding_names[i]+'Hr.txt')

    #first column - frequencies; the columns after that correspond to each point at which H was measured

    for j in range(no_f):

        #axial
        omega=2*math.pi*Hz_file[j,0]
        delta_inv = np.sqrt((omega*mu0*mur*sig)/2)
        k_ax = str_rad[i]*delta_inv
        k_rad = str_ax[i]*delta_inv
        Hz = Hz_file[j,1:]*math.sqrt(2)
        p_ax = Hz**2*(np.sinh(k_ax)-np.sin(k_ax))*delta_inv/(str_rad[i]*sig*(np.cosh(k_ax)+np.cos(k_ax)))
        P_ax[j][i] = 2*2*math.pi*t[i]*sum(p_ax*radv.flat*10**-3*w[i])*c[i]

        #radial
        omega=2*math.pi*Hr_file[j,0]
        delta_inv = np.sqrt((omega*mu0*mur*sig)/2)
        k_ax = str_rad[i]*delta_inv
        k_rad = str_ax[i]*delta_inv
        Hr = Hr_file[j,1:]*math.sqrt(2)
        p_rad = Hr**2*(np.sinh(k_rad)-np.sin(k_rad))*delta_inv/(str_ax[i]*sig*(np.cosh(k_rad)+np.cos(k_rad)))
        P_rad[j][i] = 2*2*math.pi*t[i]*sum(p_rad*radv.flat*10**-3*w[i])*c[i]
```

In [5]:
```
sum(P_ax),sum(P_rad)
```

Out[5]:
```
(array([30394.7885942 ,  7997.45074421,  1337.30476862,   920.37369001]),
 array([ 748.36397851, 9306.26800313, 9974.10650323,  742.78882175]))
```